Mechanistic Study of Enhanced Oil Recovery by Gas, WAG and SWAG Injections in Mixed-Wet Rocks: Effect of Gas/Oil IFT

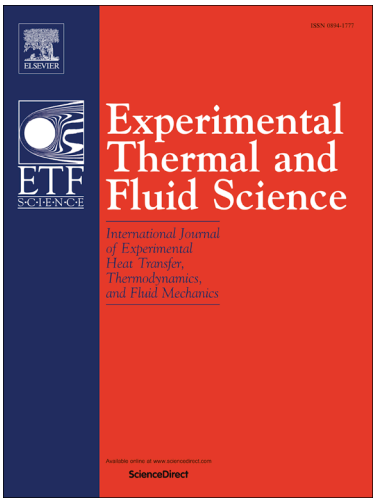

Mechanistic Study of Enhanced Oil Recovery by Gas, WAG and SWAG Injections in Mixed-Wet Rocks: Effect of Gas/Oil IFT

Mobeen Fatemi, Mehran Sohrabi

PII: S0894-1777(18)31111-7
DOI: https://doi.org/10.1016/j.expthermflusci.2018.06.011
Reference: ETF 9507

To appear in: *Experimental Thermal and Fluid Science*

Received Date: 6 August 2017
Revised Date: 8 June 2018
Accepted Date: 16 June 2018

Please cite this article as: M. Fatemi, M. Sohrabi, Mechanistic Study of Enhanced Oil Recovery by Gas, WAG and SWAG Injections in Mixed-Wet Rocks: Effect of Gas/Oil IFT, *Experimental Thermal and Fluid Science* (2018), doi: https://doi.org/10.1016/j.expthermflusci.2018.06.011

Mechanistic Study of Enhanced Oil Recovery by Gas, WAG and SWAG Injections in Mixed-Wet Rocks: Effect of Gas/Oil IFT

Mobeen Fatemi; Mehran Sohrabi

Centre for Enhanced Oil Recovery and CO_2 Solutions, Institute of Petroleum Engineering, Heriot-Watt University, UK

Abstract

We report the results of a comprehensive series of coreflood experiments carried out at three different levels of gas/oil IFT namely, ultra-low, intermediate, and high gas/oil IFT values of 0.04, 0.15, and 2.70 $mN.m^{-1}$ in mixed-wet rocks. Coreflood experiments included waterflooding (WF), gas injection (GI) and two WAG injection scenarios at each IFT value in the first series of WAG experiments, fluid injection started with water injection (I) followed by gas injection (D), and this cyclic injection of water and gas was repeated in four cycles (WAG-IDIDIDID). In the second series of WAG experiments, the test started with gas injection (D) followed by water injection (I), and this cyclic injection of water and gas was repeated four times (WAG-DIDIDIDI). In addition to these experiments, for the high and ultra-low gas/oil IFT systems, SWAG injection experiments have also been performed with SWAG ratio of unity ($Q_g/Q_w = 1$).

The results showed that the performance of GI was higher in the case of lower IFT condition compared to high-IFT system. The beneficial effect of gas/oil IFT was more pronounced in high permeable mixed-wet rock than it was in low permeable mixed-wet system. For all IFT values tested, WF performance was better than GI under mixed-wet condition. The results also showed that under mixed-wet conditions, for the three gas/oil IFT levels tested, WAG injections outperformed WF and GI. For the ultra-low IFT condition, oil recovery by the WAG-IDIDIDID experiment was higher than that of the WAG-DIDIDIDI experiment. However, at the other two IFT values, WAG-DIDIDIDI outperformed WAG-IDIDIDID injection scenario. For WAG-IDIDIDID, the lower the gas/oil IFT the higher the ultimate oil recovery; conversely, for the WAG-DIDIDIDI injection scenario, oil recovery performance was better for the high

IFT condition rather than the ultra-low IFT case. Our results show considerably higher injectivities during WF periods of the ultra-low IFT WAG injections compared to high-IF1T WAG injections. In general, injectivity was lower for the WAG-DI injection scenarios compared to the WAG-ID. The effect of gas/oil IFT on oil recovery was more significant under three-phase flow (WAG injections) compared to the two-phase flow (GI). Trapped gas saturations S_{gt} (for the same S_{gi}) were found to be higher under higher IFT conditions, and the trend of S_{gt} vs. S_{gi} curve was significantly affected by the sequence of fluid injection during WAG injection (DIDIDIDI or IDIDIDID). This is especially true for intermediate and high IFT conditions.

The results show that trapping models such as Land, Carlson, and Jerauld models cannot capture the observed trend of trapped gas saturations accurately, under the conditions of our experiments. This is especially true for the WAG-DIDIDIDI injection scenarios in which, contrary to the WAG-IDIDIDID injections, S_{gtw} values are not necessarily higher for the case with higher initial gas saturation. This shows the importance of developing new trapping models for non-water-wet systems. In addition, the results show that the reduction coefficient in S_{or} adjustment formula of the WAG-Hysteresis model (proposed by Larsen and Skauge) is a function of both gas/oil IFT and fluid injection sequence and it also depends on the rock permeability. These further highlight the importance of performing laboratory experiments under representative reservoir and operational conditions.

Introduction

Water injection is the most common method of oil recovery. Usually after water flood, significant amount of oil remains in the reservoir (S_{orw}). Part of this remaining oil can be recovered by gas injection. Various types of gas have been used for injection in oil reservoirs including, CO_2 (mostly in USA), hydrocarbon gas (mostly in the North Sea area), nitrogen and air. CO_2 and hydrocarbon gases are used in 90% of the gas injection projects worldwide (Kulkarni and Rao, 2005). To achieve a miscible flood process gas injection is operated so as to maintain the pressures above the minimum miscibility pressure (MMP). However many of the gas injection projects although designed to be miscible, are actually near-miscible displacement at reservoir conditions (Awan et al., 2008), in which injected gases do not quite

develop complete miscibility with the oil, but come close. For instance, condensing–vaporising gas drives at enrichments slightly below minimum miscibility enrichment (MME) or at pressures slightly below minimum miscibility pressure (MMP) are near-miscible processes. Near-miscible gas drives appear attractive from both economic and operational standpoints.

Nevertheless, for many oil reservoirs poor sweep efficiency has been a problem in gas injection processes. This happens due to the high gas mobility compared to that of the oil and water. Therefore, continuous gas injection may not result in economically significant additional oil recovery. In order to alleviate this problem, gas can be injected alternately with water. To improve the sweep efficiency of gas injections, Water alternating gas (WAG) injection was originally proposed to control the mobility ratio and to stabilize the propagating front (Caudle and Dyes, 1958). WAG injection is a complex form of three-phase fluid flow through porous media. Although WAG flooding has been successfully applied to many oilfields worldwide (Christensen et al., 1998), there is still an incomplete understanding of the actual mechanisms underlying oil recovery by WAG injection especially in systems with non-water-wet and non-uniform wettability (Suicmez et al., 2007). Our understanding of the performance of WAG injection and the mechanisms involved is even more limited where the oil/gas interfacial tension (IFT) is very low (near-miscible condition) (Sohrabi et al., 2004; Sohrabi et al., 2008). These are in spite of the facts that, the majority of oil reservoirs are mixed-wet or oil-wet and most of the successful WAG injection schemes involve low gas/oil interfacial tension (IFT), due to the injection gas being either high-pressure hydrocarbon gas or CO_2. From another point of view, major problem in the evaluation and prediction of WAG behaviour and effectiveness are uncertainties associated with the prediction of the relative permeabilities values of the three phases for different injection cycles which results in uncertain/erroneous performance prediction. Empirical correlations are usually used for obtaining three-phase relative permeability. However the existing predictive approaches included in commercial softwares are based on water-wet conditions and high gas/oil IFT systems (Blunt, 2000).

This has contributed to a poor performance by the existing empirical equations used for determination of three-phase relative permeabilities for non-water-wet conditions (Element et al., 2003, Shahrokhi et al.

2014). Reliable laboratory data on WAG injections under realistic reservoir conditions (i.e., mixed-wet and low gas/oil IFT) are invaluable for improved or novel three-phase relative permeability and hysteresis models to predict the complex multi-phase and multi-physics processes involved in WAG injection.

To highlight the effect of wettability, Fatemi and Sohrabi (2013a) recently reported the results of a comprehensive series of coreflood experiments (waterflood, gas injection and WAG injection) carried out for near-miscible gas/oil system in a 65 mD Clashach sandstone core under both water-wet and mixed-wet conditions (for results of the WAG experiments on oil-wet carbonate rocks see Fatemi et al.(2015)). Comparison of different experiments revealed that oil recovery by waterflood was much higher in mixed-wet system compared to the performance of water-wet sample. This is attributed to suppressed snap-off mechanism under mixed-wet conditions. Contrary to this, oil recovery by gas injection was higher for water-wet condition compared to mixed-wet. This was attributed to higher affinity of the oil phase towards the rock surfaces in mixed-wet rocks compared to that in water-wet rocks, as well as oil spreading layers in water-wet system as opposed to oil wetting layers in mixed-wet systems. Additionally, in mixed-wet rocks, the performance of gas injection was lower compared to waterflood. On the contrary, gas injection performance was considerably higher than waterflood in water-wet system. Fatemi and Sohrabi (2013a) concluded that WAG has a superior performance over both continuous water and continuous gas injection in both mixed-wet and water-wet systems. Based on their results the performance of WAG injection at ultra-low gas/oil IFT will be further improved if WAG injection begins with a water injection period, in mixed-wet rocks, and with a gas injection period in water-wet rocks.

Sohrabi and Fatemi (2012) also studied SWAG and SWAG-Tail injection scenarios for the case extra-low gas/oil IFT. The SWAG experiments were performed with two gas/water volume ratio of 0.25 and 1.0 (at test temperature and pressure). They have also investigated the effect of rock permeability on the performance of different injection scenarios for a 65 mD rock sample and a 1000 mD rock. The results showed that in both mixed-wet cores, WAG injection performed better than SWAG injection. SWAG

performed better compared to GI. However, surprisingly, SWAG resulted in lower oil recovery compared to waterflood in their mixed-wet systems. It was observed that increasing the gas/water ratio in SWAG leads to faster gas breakthrough, higher produced gas/oil ratio and further reduction in the performance of SWAG. SWAG-Tail injection strategies (gas and/or WAG injection after SWAG injection) didn't improve oil recovery considerably.

To further investigate different gas injection scenarios in mixed-wet systems, the objective of the present work is, firstly, to extend our previous studies to intermediate and high gas/oil IFT conditions. This helps to better understand the effect of recovery mechanisms on the core-scale (injectivity and production data) behaviour of the system and to investigate the effect of gas and oil properties on the performance of WF, GI, WAG and SWAG injections. Secondly, to generate reliable experimental data for estimation of three-phase relative permeabilities (Fatemi and Sohrabi, 2012a; Fatemi and Sohrabi, 2013b) under different pertinent conditions. These presented experiments would also be vital for a proper assessment of the formulations available in commercial reservoir simulators for accounting the hysteresis taking place in WAG injection (Fatemi and Sohrabi (2013e); Shahrokhi et al., 2014). For the required two-phase relative permeabilities and capillary pressures data to evaluate the performance of the hysteresis models against the experimental data set presented in this work see Fatemi et al (2012), Fatemi and Sohrabi (2012b, 2013c); Fatemi and Sohrabi (2018). The presented experimental data can also be used to develop improved (Shahrokhi et al., 2014) or novel methodologies (Duchenne et al 2016) for predicting three-phase relative permeabilities and hysteresis models.

Materials

Rock Properties

A Clashach sandstone core with an absolute permeability of 65 mD was used in this study. Table 1 shows the physical properties of this core sample. The wettability of the core was changed from water-wet to mixed-wet by aging in a suitable crude oil. Mixed-wettability was confirmed with SEM images of the thin sections of the similar core undergone similar procedures. Also using Semi-Dynamic capillary

measurement technique, the USBM index showed global neutral-wet behaviour for the rock after aging (Fatemi, 2015).

In all the reported experiments, the immobile water saturation was established at the beginning of each test and its quantity and variation along the core was obtained by material balance and by x-ray scanning to make sure that it remained the same in all the tests.

Table 1: Physical properties of the 65mD mixed-wet core sample.

Property	***Value***	***Property***	***Value***
Length	60.5 cm	K_{abs}	65 mD
Diameter	5.082 cm	Φ	18.2 %

Fluids

Fluids used in the experiments are water, gas and oil. The brine (water phase) used in the tests was synthesized using NaCl and $CaCl_2$ in distilled and degassed water (16 g sodium chloride (NaCl) and 4 g calcium chloride ($CaCl_2$) for 2000 cm^3 of degassed distilled water). The hydrocarbon fluid system used in the coreflood experiments is prepared from a binary mixture of methane and n-butane. To eliminate mass transfer during the displacement experiments, all the fluids (oil, gas, and brine) were pre-equilibrated at average (mid core) test pressure and temperature, and were kept under equilibrium at these conditions in high pressure transfer vessels kept in a temperature controlled oven. Mixing was repeated several times prior to each experiment to ensure that phase equilibrium conditions were satisfied. Table 3 shows the measured properties of this fluid system at the test temperature, 38 ºC (100 ºF), and different test pressures (corresponding to different gas/oil IFT values). Since the critical pressure of this hydrocarbon mixture at 38 ºC (100ºF) is about 12.86 MPa (1865 psia), at 12.69 MPa (1840 psia) the pressure is very close to its critical point and hence, the gas and oil are nearly miscible (extra-low gas-oil IFT, ~ 0.04 mNm^{-1}). At pressure of 12.34 MPa (1790 psia), gas/oil IFT is 0.15 $mN.m^{-1}$ and this condition will be considered as intermediate IFT system, compared to the tests at pressure of 8.27 MPa (1215 psia) in which the gas/oil system will be considered as immiscible (IFT_{o-g} = 2.7 mNm^{-1}). More details on the physical properties of the gas/oil system, wettability alteration procedure and immobile water establishment and its evaluation using x-ray can be found elsewhere (Fatemi and

Sohrabi 2013a; Fatemi, 2015).

Table 2: physical properties of synthetic brine used in experiments

Salinity (mg/L)	Density @ 38°C (gr/L)	Viscosity @ 38°C (cp)
10000	992.96	0.68

Table 3: measured fluid properties for C1-nC4 binary mixture at 38 ºC.

Pressure /psia	ρ_g /kg.m^{-3}	ρ_L /kg.m^{-3}	μ_g /mPa.s	μ_L /mPa.s	IFT /mN.m^{-1}
1215	86.68	466.06	0.0141	0.0793	2.70
1790	184.8	345.10	0.0206	0.0474	0.15
1840	211.4	317.40	0.0249	0.0405	0.04

Methodology

Table 4 summarizes the list of the experiments performed previously on the 65mD mixed-wet core using ultra-low gas/oil IFT fluid systems (Fatemi and Sohrabi, 2013a), which will be used in this paper as well. For details of each experiment refer to the original paper.

Table 5 summarizes the list of the new experiments performed on the same 65 mD mixed-wet core but at intermediate and high gas/oil IFT conditions. The experimental condition is constant injection rate and constant average pressure condition (this means that the production rate is adjusted so that the average core pressure will be constant and equal to the initial core pressure during the experiment. As explained in Fatemi and Sohrabi (2013a), the initial water saturation is established with the same procedures but with mineral oils which had much higher viscosities than all of the oils used in this study as oil in place. As a result the value of the S_{wi} is independent of the oil used in the actual tests.

It should be mentioned that the injected period and WAG ratio would affect the ultimate oil recovery. In this study we continued 1st gas injection period (in WAG-ID scenario) until there is no considerable amount of oil production, and then we switched to 2nd water injection and continued WF till reached to residual oil saturation. Since for water injection periods the residual oil and gas saturations occurred at less injected volume compared to the previous gas injection, we can assume that the WAG ratio is equal

to 1 (further injection of the water wouldn't change the saturations inside the core). The design of the experiment was then so to keep the gas injection periods the same, yet to inject the following water period till the residual saturations (which again happened at smaller injected volumes compared to preceding gas injection). Regarding the smaller injection periods and its possible effect see Alkhazmi et al. (2017). Based on their results although, the size of slugs affected the performance of either WAG-ID or WAG-DI injection scenarios, yet the the WAG-DI outperformed WAG-ID and both had better performance compared to the WF and GI. It should be mentioned that in this study we have investigated the pure effect of displacement mechanism. This shows that the displacement efficiency of the front, and make it possible for us to use the experimental data (which are not affected by any other parameter such as gravity or mass transfer) for obtaining reliable relative permeability data. As a result, in actual reservoir condition the effectiveness of the various water and gas injection methods might be different due to gravity segregation, heterogeneity, mass transfer especially between gas and oil phases and etc. These sorts of effects are predictable and can be captured by advanced simulations once you got reliable relative permeabilities to predict the flow behaviour of different phases.

Table 4: List of the coreflood experiments performed in 65 mD mixed-wet sandstone at 1840 psia (Fatemi and Sohrabi, 2013a; Sohrabi and Fatemi, 2012)(Q_{inj} = 25 $cm^3.hr^{-1}$, S_{wim} = 0.18)..

#	Experiment	Direction	Gas/oil IFT ($mN.m^{-1}$)
1	Gas Injection	Drainage	0.04
2	Water Injection	Imbibition	---
3	WAG	IDIDID	0.04
4	WAG	DIDIDIDI	0.04
5	SWAG $_{(Qg/Qw=0.25)}$	(So↓, Sw↑, Sg↑)	0.04
6	SWAG $_{(Qg/Qw=1)}$	(So↓, Sw↑, Sg↑)	0.04

Table 5: List of the coreflood experiments performed in 65 mD mixed-wet sandstone presented in the current study (Q_{inj} = 25 $cm^3.hr^{-1}$, S_{wim} = 0.18).

#	Experiment	Direction	Gas/oil IFT ($mN.m^{-1}$)
7	Gas Injection	Drainage	0.15
8	Gas Injection	Drainage	2.70
9	WAG	IDIDID	0.15
10	WAG	DIDIDIDI	0.15
11	WAG	IDIDID	2.70
12	WAG	DIDIDIDI	2.70
13	SWAG $_{(Qg/Qw=1)}$	(S_o↓, S_w↑, S_g↑)	2.70

Considering the fact that these tests are very time consuming, almost 1 month core preparation and 1-1.5 month performing the WAG test itself (Fatemi and Sohrabi, 2013a), we have been unable to repeat all of these tests due to time frame of the project, but we have repeated some of the key ones. For example gas injection at extra low IFT have been performed three times in mixed-wet system, once was repeated immediately after the 1st experiment to make sure that the production and Dp data are recorded correctly, and another time after almost 1.5 years or so, to make sure about the wettability condition of the core (for details refer to Fatemi (2015)). Also please note that 1st gas injection in WAG-DI and 1st water injection in WAG-ID tests have the same trend as the extended GI and WF tests, which also confirms the repeatability of the tests.

Extended Gas Injection, 1790 psia, gas/oil IFT = 0.15 mN.m^{-1}

Gas injection started in the core with water and oil saturations of S_{wim}=18% and S_{oi}=82%. The gas injection began at 25 cm^3.hr^{-1} (at 1790 psia and 38 °C) and continued for around 13 PV. It should be mentioned that oil production continued after the gas breakthrough (although at lower rates). Oil and gas saturations at the end of the gas injection period as calculated from material balance were 25.2% and 56.8%, respectively.

Extended Gas Injection, 1215 psia, gas/oil IFT = 2.70 mN.m^{-1}

Prior to performing this gas injection, oil saturation of 82% was first established in the core (with 18% irreducible water). Then, the equilibrated gas was injected through the core at 1215 psia and 38 °C. The gas breakthrough (BT) took place after 0.27 PV injections. Oil production didn't cease after the gas breakthrough, and continued (although at small rates) until the end of the coreflood. The gas injection continued for an extended period of time and after around 8.24 PV of gas injection the residual oil saturation was approximately 31%.

WAG-IDIDID, 1790 psia, gas/oil IFT = 0.15 mN.m^{-1}

This WAG injection started with water flooding. Three periods of water injection (Imbibition, identified

by I) followed by gas injection (Drainage, identified by D) were carried out (termed: WAG-IDIDID or simply WAG-ID injection scenario). The first water injection period continued for around 2.5 PV. The oil and water saturations at the end of this water injection period, as calculated by material balance were 27.1% and 72.9%, respectively.

Figure 1 shows oil recovery (as a fraction of core PV), for all the three cycles (IDIDID) of WAG injection, performed at 1790 psia (12.34 MPa). Oil recovery for each period of injection (water or gas) has been separated by a dashed line and an abbreviation of that coreflood (W for water injection and G for gas injections). This Figure shows that at the end of 1st water flooding almost 55% of core PV (67 % of the initial oil in place, IOIP) which is different from core PV) was recovered. The ultimate oil recovery achievable by WAG injection after three cycles of injection was 60% of core PV (73 % of the IOIP). Figure 2 shows oil, gas and water saturations change during this WAG injection test at this intermediate gas/oil IFT. As the alternation between water and gas injections continue the initial gas saturation (S_{gi}) at the start of water injection stages as well as trapped gas saturations at the end of water injection periods increase.

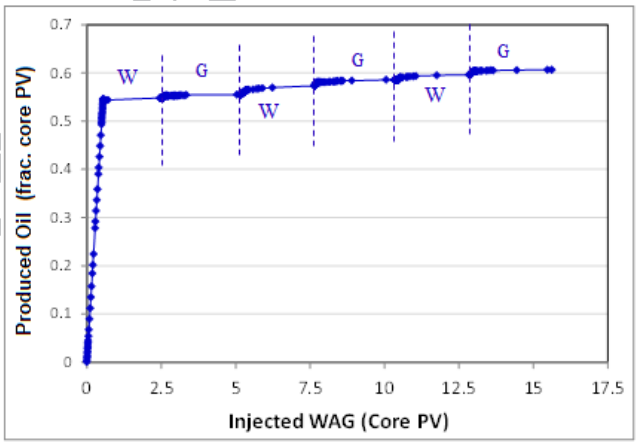

Figure 1: Produced oil vs. PV WAG injected (WAG-ID, gas/oil IFT = 0.15 mN.m^{-1}, 65mD, mixed-wet).

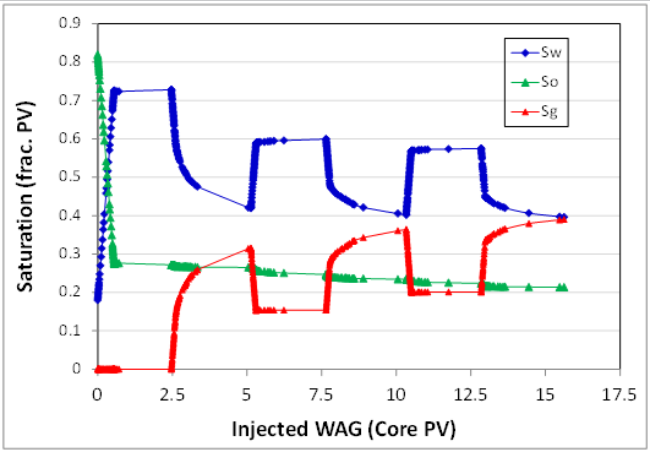

Figure 2: Average oil, gas and brine saturations vs. PV WAG injected (WAG-ID, gas/oil IFT = 0.15 mN.m^{-1}, 65mD, mixed-wet).

WAG-DIDIDIDI, 1790 psia, gas/oil IFT = 0.15 mN.m^{-1}

This series of tests started with a gas injection (Drainage: D) into the core which was followed by a water injection, i.e., an imbibition period (I). The stages of gas and water injections were repeated and in total four cycles of injections were performed (WAG-DIDIDIDI or simply WAG-DI). The initial gas injection continued for about 2.65 PV. Comparing pressure drop across the core and recovered oil for the 1st gas injection period of the WAG-DI injection scenario, with those of the extended gas injection (both for gas/oil IFT = 0.15 mN.m^{-1}) shows excellent repeatability of the experiments (Fatemi 2015).

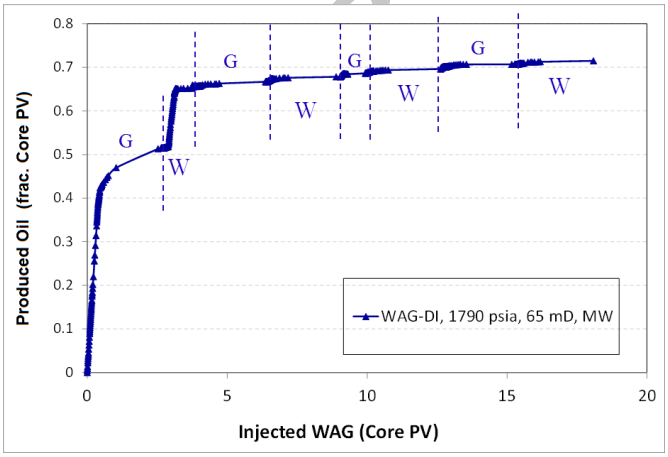

Figure 3 shows oil recovery (as a fraction of core PV) for this WAG-DI injection scenario performed at gas/oil IFT = 0.15 mN.m^{-1}. This Figure shows that after 2.65 PV injection of 1st gas injection almost 51.5 % of Core PV is recovered (62.8 % of the IOIP). Changing the injection from 1st gas injection to

water injection significantly improved oil production and the final oil recovery was 65.2 % of Core PV (79.5 % of IOIP) which means additional 16.7 % of IOIP for the 2nd period of injection. The ultimate oil recovery achievable by the complete WAG-DI injection scenario after 4 cycles of injection was 71.5 % of Core PV (87.2 % of the IOIP). Figure 4 shows average saturations of oil, gas and water during this WAG-DI injection scenario at gas/oil IFT of 0.15 mN.m^{-1}. This Figure shows that for the successive water injection periods, trapped gas saturation (S_{gt}) increased. This manes that S_{gt} at the end of 4th water injection period is higher compared to the 3rd period of water injection and so on ($S_{gt}^{W4} > S_{gt}^{w3} > S_{gt}^{w2} > S_{gt}^{w1}$).

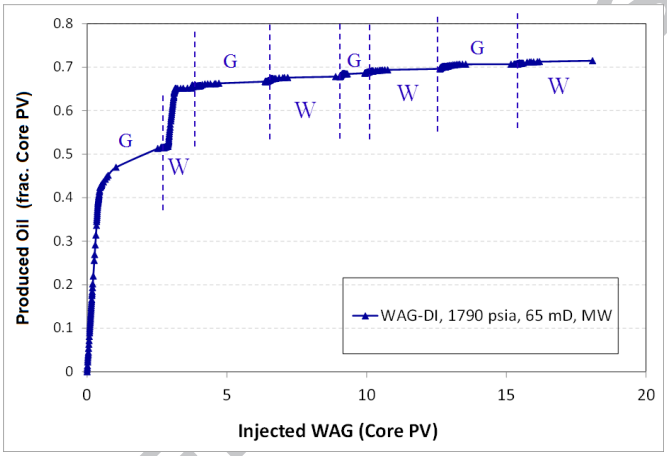

Figure 3: Produced oil vs. PV gas and water injected (WAG-DI, gas/oil IFT = 0.15 mN.m^{-1}, 65mD, mixed-wet).

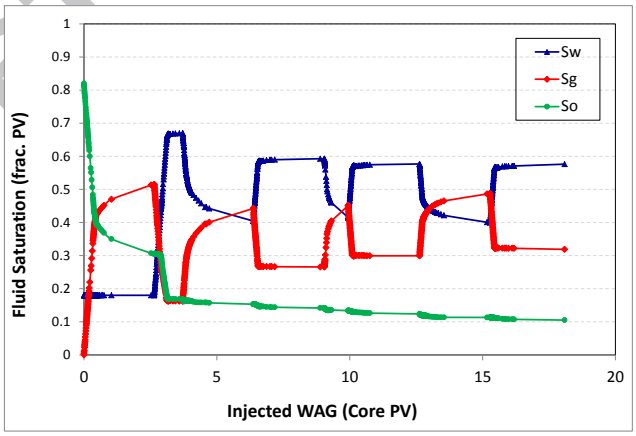

Figure 4: Average saturations of gasoil and brine vs. PV gas and water injected (WAG-DI, gas/oil IFT = 0.15 mN.m^{-1}, 65mD, mixed-wet).

WAG-IDIDIDI, 1215 psia, gas/oil IFT = 2.70 mN.m^{-1}

Figure 5 shows oil recovery as a function of PV brine and gas injected into the core during the WAG test

performed at 1215 psia ($IFT_{o/g}$ = 2.70 $mN.m^{-1}$). 1st waterflooding produced 51 % of the core PV (62% of IOIP). The additional oil recovery (fraction of IOIP) during the next 11 PV of the WAG injection (alternating injection of the gas and water) is just 4%. Figure 6 shows water, gas and oil average saturations inside the core during this WAG injection. As the alternation of water and gas injection continues, trapped gas saturation (at the end of water injections) increases. S_{gtw} has increased from 11% at the end of 2nd water injection to 14% after 3rd water injection. This shows that although the WAG injection is still working in terms of trapping the injected gas, but for the case of these immiscible gas injections, the high viscosity difference between oil and gas makes it impossible for gas to produce significant additional oil recovery in tertiary mode.

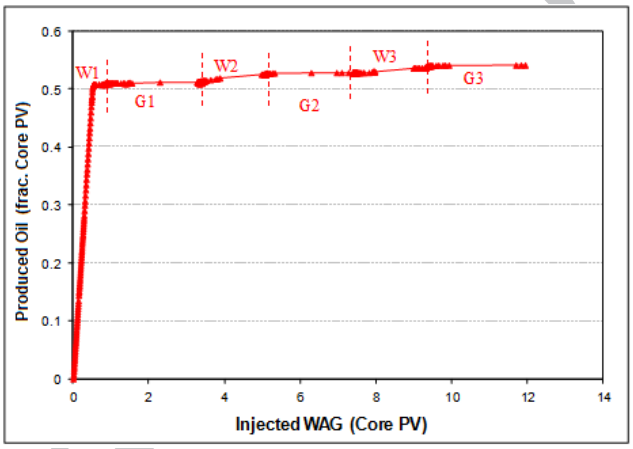

Figure 5: Produced oil vs. PV WAG injected (WAG-ID, IFT $_{o/g}$ = 2.70 $mN.m^{-1}$, 65mD, mixed-wet).

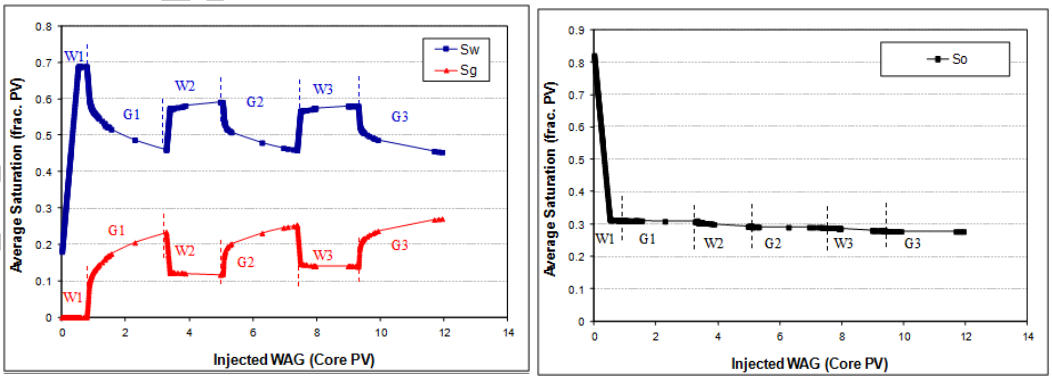

Figure 6: Water, gas and oil average saturations Oil recovery vs. PV WAG injected (WAG-ID, IFT $_{o/g}$ = 2.70 $mN.m^{-1}$, 65mD, mixed-wet).

WAG-DIDIDIDI, @ 1215 psia, gas/oil IFT = 2.70 $mN.m^{-1}$

Comparing the pressure drop across the core and recovered oil for the 1st gas injection period of the

WAG-DI injection scenario with the extended gas injection (both for gas/oil IFT = 2.70 $mN.m^{-1}$), showed excellent repeatability for the immiscible gas injection (Fatemi 2015). Figure 7 shows oil recovery (as a fraction of core PV), for this DIDIDIDI injection scenario performed at gas/oil IFT = 2.7 $mN.m^{-1}$. This Figure shows that at the end of primary gas flooding almost 47 % of core PV (57 % of the IOIP) is recovered. Alternation of injection from 1st gas injection to water injection significantly improved oil production with a remarkable final oil recovery of 89 % of IOIP (additional 32 % of IOIP). The ultimate oil recovery achievable by complete DIDIDIDI injection scenario after 4 cycles of injection was 76.2 % of core PV (93 % of the IOIP). Figure 8 shows shows that although initial gas saturation (S_{gi}) at the start of 1st water flooding is higher than successive water injection periods, yet the trapped gas saturation is lower for this period of injection than those observed in the successive water injection periods. The same graph shows that trapped gas saturations remain almost constant for the 2nd, 3rd and 4th water injection periods.

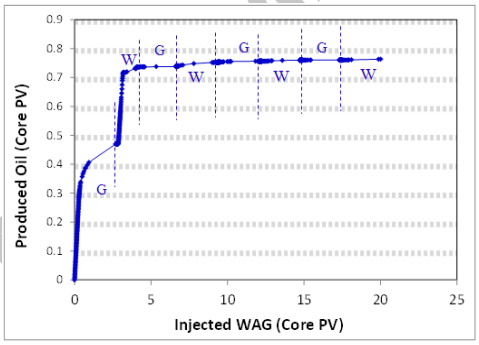

Figure 7: Produced oil vs. PV gas and water injected (WAG-DI, gas/oil IFT = 2.7 $mN.m^{-1}$, 65mD, mixed-wet).

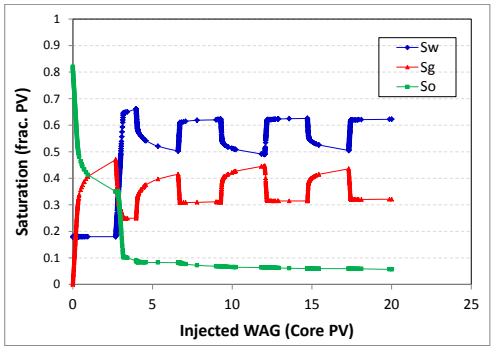

Figure 8: Average oil, gas and brine saturations vs. PV gas and water injected (WAG-DI, gas/oil IFT = 2.7 $mN.m^{-1}$, 65mD, mixed-wet).

SWAG injection with Q_g/Q_w=1.0, @ 1215 psia, gas/oil IFT = 2.70 mN.m^{-1}

Having established an initial oil saturation of 82% and water saturation of 18% at 1215 psia (corresponding to gas-oil IFT of 2.70 mN.m^{-1}), water and gas were simultaneously injected through the core. Water was injected at the rate of 12.5 cm^3.h^{-1} and gas was injected at the same rate (total fluid injection rate of 25 cm^3.h^{-1}) i.e., at a SWAG ratio of 1.0 (cm^3/cm^3 both at 1215 psia and 38^{o}C). The SWAG injection was continued until almost 5.2 PV of fluids had been injected. With the start of the SWAG injection, pressure drop across the core starts increasing. After 0.44 PV SWAG injections, gas breakthrough (BT) at the outlet was observed. The increase in ΔP continues even after gas BT. While water and gas are (simultaneously) injected through the core, only oil is being recovered from the core up until around 0.44 PV of SWAG injections. After gas breakthrough, gas and oil are both being produced from the core. The quicker breakthrough of gas compared to the water phase (which has taken place at 0.84 PV injections of SWAG) happens due to the higher mobility of this phase. The slope of the oil production curve decreases slightly after the gas breakthrough. With the breakthrough of water, pressure drop increase slows down but it remains significant till the end of this coreflood (5.2 PV injections). There is no significant oil recovery after water BT (around 2% additional oil recovery for 4.36 PV injections). Figure 9 shows average saturations of the three phases (gas, oil and water) during this SWAG injection test. With the start of the test, gas and water saturations inside the core rise along with oil production (oil saturation decreases). After gas BT gas saturation remains almost unchanged till water BT. In this period (between the two BT points), the amount of injected gas is equal to the produced gas and water is displacing oil out of the core. After water BT, water and oil saturations decrease slightly while gas saturation inside the core increases, which means that gas is displacing oil and water out of the core (although at very small rates). This is probably the reason that the pressure drop continues to rise even after gas breakthrough.

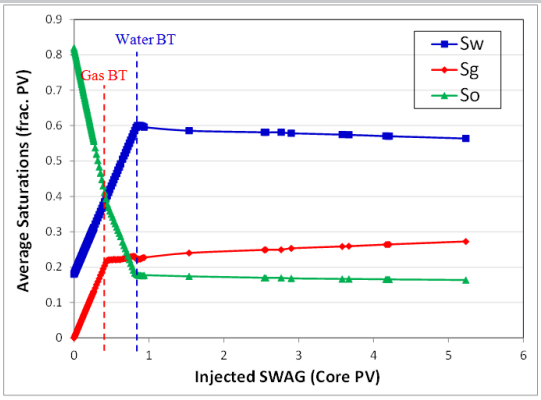

Figure 9: Average saturations inside the core during SWAG injection (immiscible gas/oil system, Q_g/Q_w=1.0, 65mD, Mixed-Wet)

Discussion

Effect of Gas/Oil IFT on the Performance of Extended Gas Injections

Figure 10 shows a comparison of oil recovery for the intermediate IFT gas injection (gas/oil IFT = 0.15 $mN.m^{-1}$) with those of near-miscible gas injection (ultra-low IFT = 0.04 mNm^{-1}) and immiscible gas injection (high IFT= 2.7 $mN.m^{-1}$), all performed in 65 mD mixed-wet core. It can be seen that gas breakthrough happened earlier in immiscible gas injection compared to the near-miscible gas injection. Interestingly, the gas breakthrough time is almost identical for the intermediate IFT gas injection of 0.15 $mN.m^{-1}$ and ultra-low IFT gas injection of 0.04 $mN.m^{-1}$. However, after gas breakthrough, the oil production rate (as indicated by the slope of the recovery curve) is lower for gas injections performed at 1215 psia and 1790 psia compared to the gas injection test performed at 1840 psia. The difference between the oil recoveries of the two gas injections performed at 1840 psia and 1790 psia grew after the breakthrough as the injection proceeded. However the difference between the two gas injections performed at 1790 psia and 1215 psia remained almost the same towards the end of the experiments.

Figure 11 shows the comparison of the oil recovery for the near-miscible gas injection and the immiscible gas injection, both performed in the 1000 mD mixed-wet core. It can be noted that the

difference between oil recoveries at the breakthrough points as well as the final oil recoveries of the low and high IFT cases are larger in 1000 mD core compared to 65 mD core. Unfortunately, for the 1000 mD core sample, no gas injection has been performed at the intermediate gas/oil IFT condition. By comparing the results of the two core samples, it is obvious that the effect of IFT is pronounced for the 1000 mD sample. In other words, the gain in recovery obtained by raising the pressure (reducing IFT), is more in high permeability core than it is in the low permeability core.

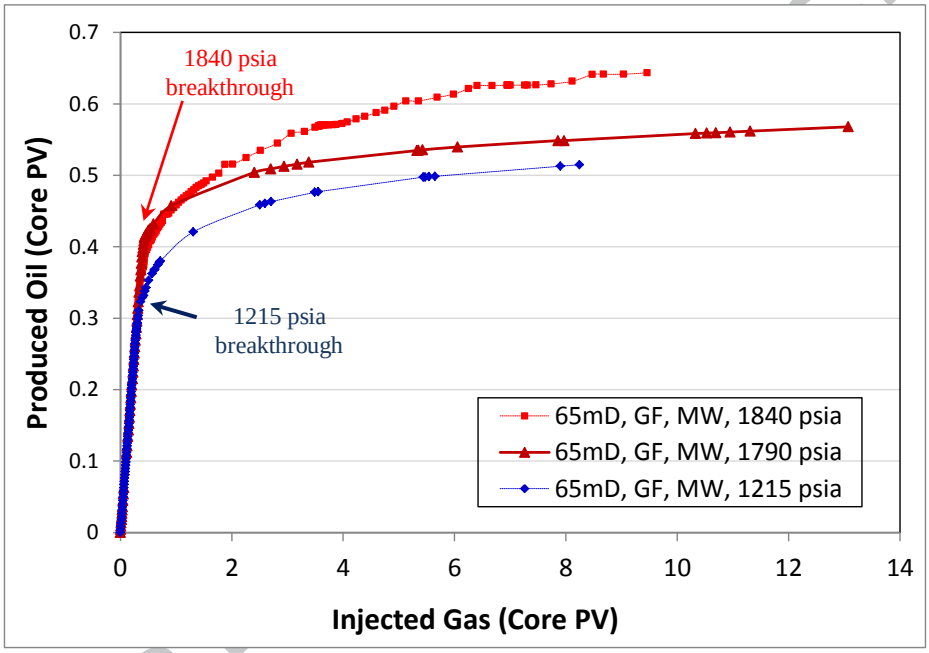

Figure 10: produced oil vs. injected gas pore volume (extended gas Injection, IFT = 0.04 at 1840 psia, 0.15 at 1790 psia, and 2.70 mN.m^{-1} at 1215 psia, 65 mD, mixed-wet).

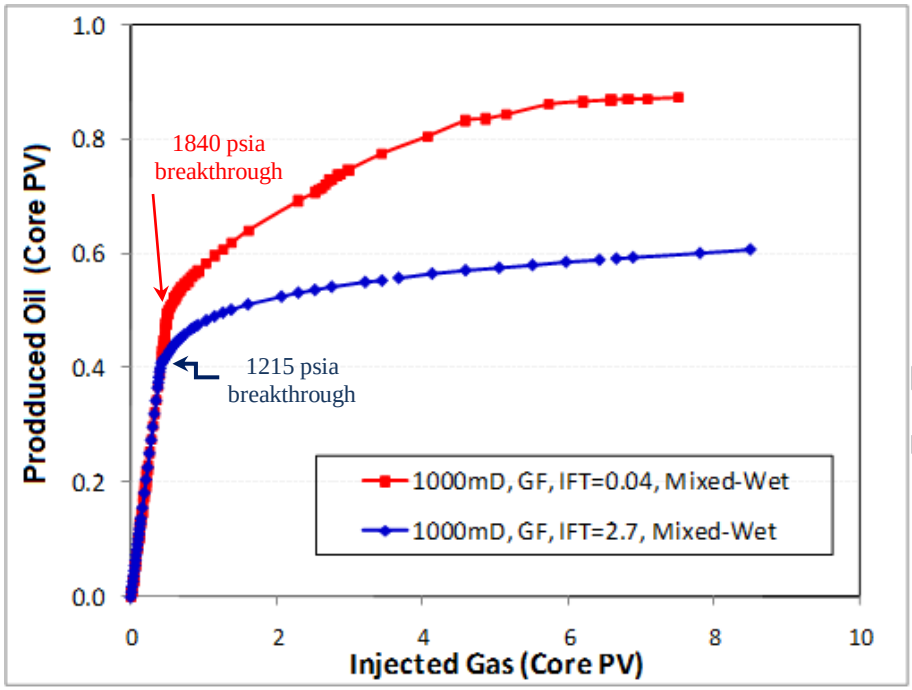

Figure 11: Produced oil vs. injected gas pore volume (extended gas Injection, IFT = 0.04 mN.m^{-1}at 1840 psia, vs. 2.70 mN.m^{-1}at 1215 psia, 1000 mD, mixed-wet).

Effect of Gas/Oil IFT on the Performance of WAG-ID Injections

In Figure 12, the left graph compares the oil recovery factor (fraction of IOIP) for the case of three WAG injections started with waterflooding, performed under different gas/oil IFT conditions (different test pressures). The same figure also includes the difference between the oil recoveries during the 1st water injection stage. It is worth mentioning that viscosities of the oil phases in these cases are different. For the test performed at 1840 psia, viscosity of oil was 0.0405 cp while in the case of 1215 psia tests, the oil viscosity was 0.0793 cp, which is almost twice the former value. In line with viscosity values, the pressure drop across the core is almost twice for the primary waterflooding at 1215 psia compared to the primary waterflooding at 1840 psia (12.69 MPa). Contrary to this, at the test pressure of 1790 psia the oil viscosity is very close to the 1840 psia (0.0474 cp compared to the 0.0405 cp). Figure 12, left graph, shows that there is a trend between test pressure and the performance of the 1st water injection. This means that recovered oil is higher for the case with higher pressure (less viscous oil). In fact, the oil recovery in the case of the highest oil viscosity (1215 psia) is almost 15% (% IOIP) less than the case with lowest viscosity (1840 psia). Interestingly, although the ΔP for the case of WF at 1790 psia is very

close to those of WF at 1840psia, yet the recovered oil is closer to those of the WF performed at 1215 psia.

We believe that this is partly due to the composition differences between the oil samples at these pressures (Table 3). At 1840 psia the oil sample has more dissolved C1 compared to the one at 1790 psia (which in turn has more dissolved C1 than the oil sample at 1215 psia) (see Gozalpour et al 2005). This would result in a sort of "apparent" wettability differences (although the actual wettability of the system is unchanged) (Fahimpour and Jamiolahmady (2014)). It should be mentioned that this is different from the spreading criteria which is usually defined for three-phase systems as opposed to the two-phase oil/water system discussed here. The differences in apparent wettability are the result of the difference in the affinity of the oil phase towards the rock grains' surfaces in the non-water wet systems. The performed contact angle tests by Fahimpour and Jamiolahmady (2014) demonstrated that the performance of wettability alteration for the same hydrocarbon system as used in this study is highly dependent on the molecular composition of the hydrocarbon phase and the thermodynamic conditions. Overall, it was found that the oil wetting tendency on the treated surface considerably increased as IFT decreased (oil becomes heavier). In conjunction to our study the oil sample with highest C1 content acts more like a gaseous phase than oil phase (@ 1840 psia), and the one with lowest C1 content (@1215 psia) act more like heavier oil phase. As a result, the oil/water phase at 1840 psia behaves like neutral-wet system, while the oil/water phase at 1215 psia behaves close to oil-wet system. Oil/water system at 1790 psia behaves in between i.e. slightly oil-wet (since the C1/C4 composition of the oil is between the other two extremes (see Gozalpour et al 2005)). This would result in the differences in oil recoveries due to -apparent- wettability and the outcome is similar to what we have reported in our previous study for the effect of actual wettability (water-wet vs. mixed-wet), on the recovery of a specified oil composition (Fatemi and Sohrabi, 2013a). Further investigation regarding the effect of oil composition on the oil recovery and apparent wettability in non-water wet systems is in progress at this time to better understand this concept from molecular point of view.

Figure 12, left graph, confirms significant higher oil recovery (as fraction of the initial oil in place) for

the WAG-ID performed at near-miscible gas/oil condition (1840 psia) compared to the tests performed at lower pressures (higher gas/oil IFTs). To further highlight the differences between the performances of these WAG injections after primary water injection, in the right graph of Figure 12, the recoveries are presented as fraction of the residual oil at the end of primary water-flooding. Although the gas/oil IFT for the case of the test performed at 1790 psia is as low as 0.15 $mN.m^{-1}$, yet the 1st gas injection does not significantly enhance the oil production, compared to the near-miscible gas injection (gas/oil IFT = 0.04 $mN.m^{-1}$). In fact, performance of the 1st gas injection at gas/oil IFT of 0.15 $mN.m^{-1}$ is much closer to the case of immiscible condition, than it is to the recoveries of the near-miscible case.

With the start of the 1st gas injection (tertiary in this case), water saturation decreases as the gas displaced it in a piston like pore-body filling manner at pore-scale (compared to the film like encroachment and snap-off mechanism) (see Sohrabi et al., 2004; 2008) . As the gas injection is continued and water saturation is sufficiently decreased, the injected gas comes closer in contact with the oil. For the case of near-miscible WAG injection, oil can flow along with gas even behind the gas front (μ_o/μ_g = 1.62), which results in significant additional oil recovery after breakthrough during the tertiary gas injections. For the immiscible WAG injection, the gas viscosity is much lower than that of oil (μ_o/μ_g = 5.62) and recovery mechanism (at pore-scale) is more of a piston like displacement which is ineffective during tertiary gas injection. For the intermediate gas/oil IFT condition in which μ_o/μ_g = 2.30, WAG injection recovery profile is closer to that of the immiscible case. This confirms the importance of extra low IFT which makes the simultaneous flow of the residual oil and gas possible in the same pore (similar to the coupling effect as discussed by Henderson et al. (2000)).

Figure 13 compares ternary diagrams of the saturations paths for these three WAG-ID injections, which also shows that the saturation path of the test performed at 0.15 $mN.m^{-1}$ is closer to the 2.70 $mN.m^{-1}$ WAG injection than to the case of 0.04 $mN.m^{-1}$. It should be mentioned that unlike most of the immiscible WAG experiments reported in literature, here we have pre-equilibrated the three fluid phases. As a result, the reported oil recovery here is mainly due to the displacement at pore scale, and there is no effect of variations in gas solubility, swelling or miscibility variations along the core, which

could exist in many of the miscible or immiscible injection cases reported in literature.

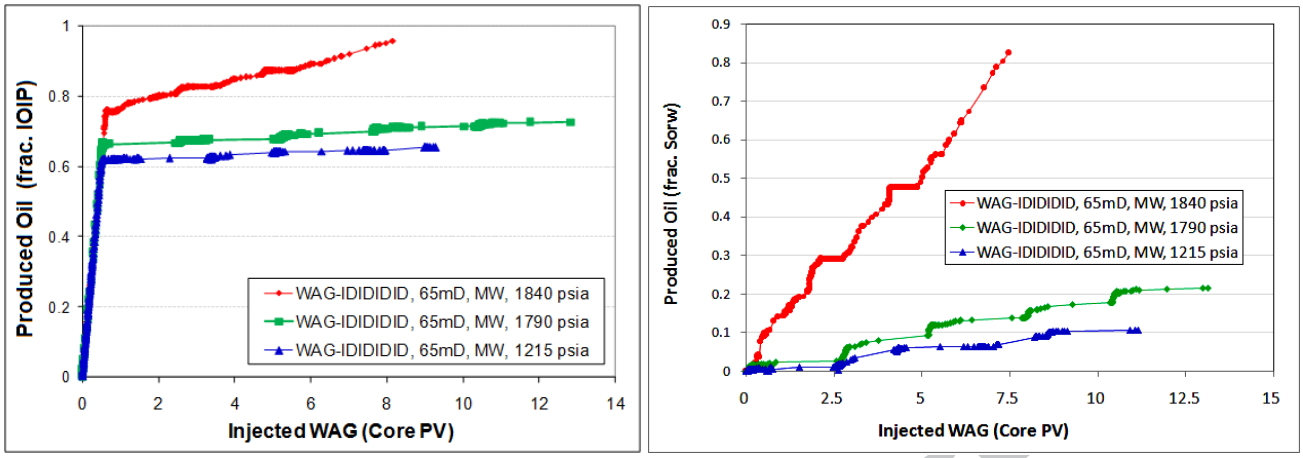

Figure 12: Comparison of produced oil for the WAG-ID injections performed at different gas/oil IFT (65mD, mixed-wet).

Figure 14 compares the injectivities (injection rate divided by pressure drop across the core) calculated during different water injection periods of these three WAG injections performed at 1840 psia top chart, 1790 psia, middle chart, and 1215 psia, lower chart. Comparison of the pressure drop data during tertiary water injections (three-phase, identified by W_2 and W_3) with those of the primary water injection (two-phase, primary water flood, identified by W_1) shows that for both $IFT_{g/o}$ = 0.15 $mN.m^{-1}$ and 2.70 $mN.m^{-1}$ WAG injections, water injectivity significantly decreased (pressure drop increased) in the three-phase flow cases (W_2 and W_3) compared to the two-phase flow (W_1). Although this trend is also observable for the WAG-ID injection performed at near-miscible condition, IFT = 0.04 $mN.m^{-1}$ (top chart); however, the reduction of the injectivity (increase of the pressure drop) is negligible compared to the other two WAG injections (middle and bottom charts).

Figure 15 compares the residual oil saturations obtained from water injection stages of these three WAG injection tests. It should be noted that for all systems the residual oil saturation corresponding to the highest initial oil saturation (S_{oi} = 82 %) is in fact the two-phase residual oil saturation at the end of 1st period of water injection (primary waterflood). Thus, the three points with S_{oi} = 0.82 correspond to the absolute possible limit of the three-phase residual oil saturation in which gas saturation, at least theoretically, has vanished (since in the presence of immobile water saturation (S_{wim} = 18 %) and S_{oi} = 82 % there will be no gas in the system). As expected, the Figure shows that residual oil saturation is

larger in the case of immiscible WAG injection compared to the near-miscible WAG injection, and residual oil values for the intermediate pressure lie between the two extreme conditions. From the trend of data, the difference between the three systems becomes less for S_{oi} values less than 30%.

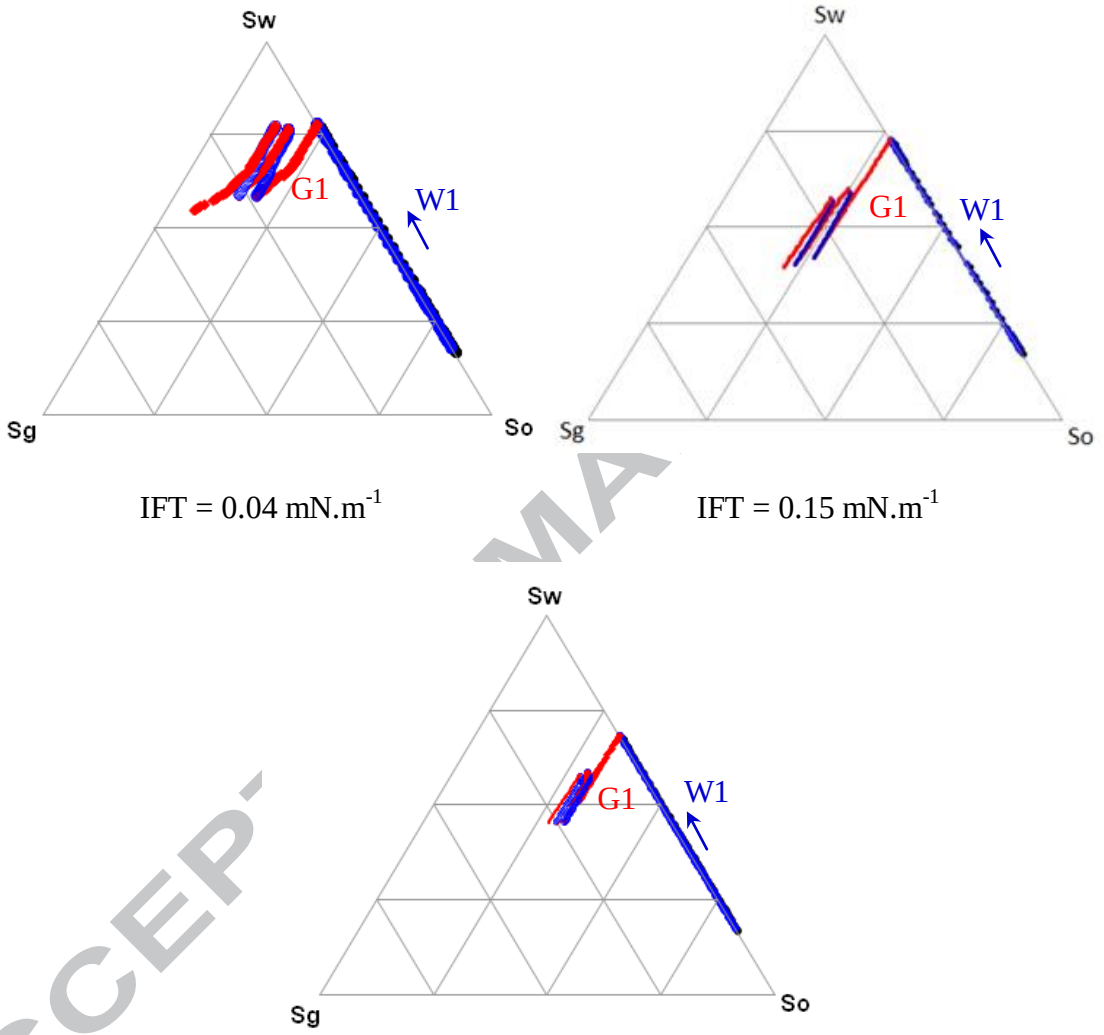

*Figure 13: Ternary diagram of saturations' changes for the WAG injections performed at different gas/oil IFT (65mD, WAG-ID, mixed-wet; from left and top to bottom: near miscible, intermediate and immiscible gas/oil systems.(red: gas injection, **blue**: water injection).*

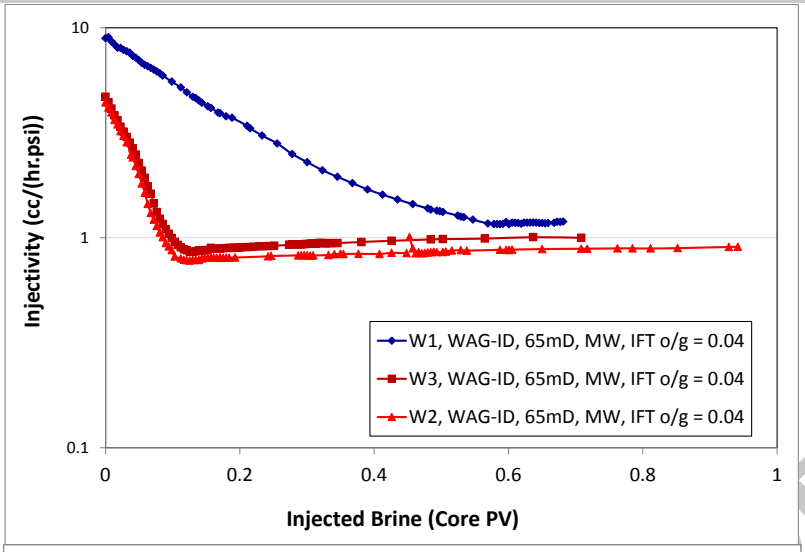

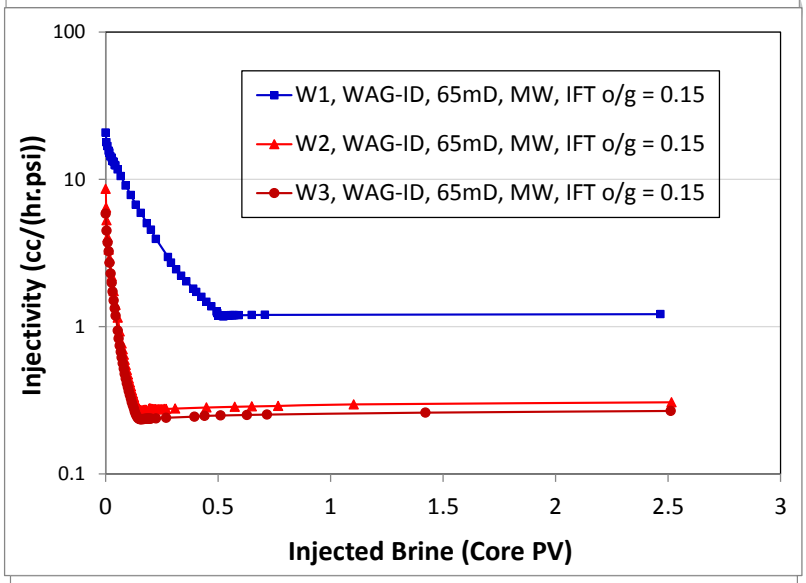

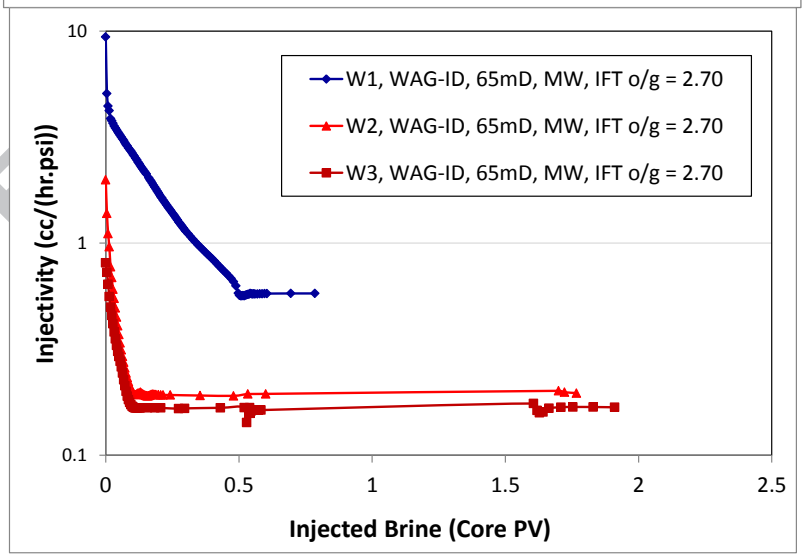

Figure 14: Comparison of the injectivities for different periods of water injection of the WAG-ID injections performed at different gas/oil IFT conditions (65 mD, WAG-ID, mixed-wet, from top to bottom: $IFT_{o/g}$ = 0.04 $mN.m^{-1}$, $IFT_{o/g}$ = 0.15 $mN.m^{-1}$ and $IFT_{o/g}$ = 2.70 $mN.m^{-1}$). W_1, W_2 and W_3 refer to the 1st (i.e., primary), 2nd and 3rd stages of water injection.

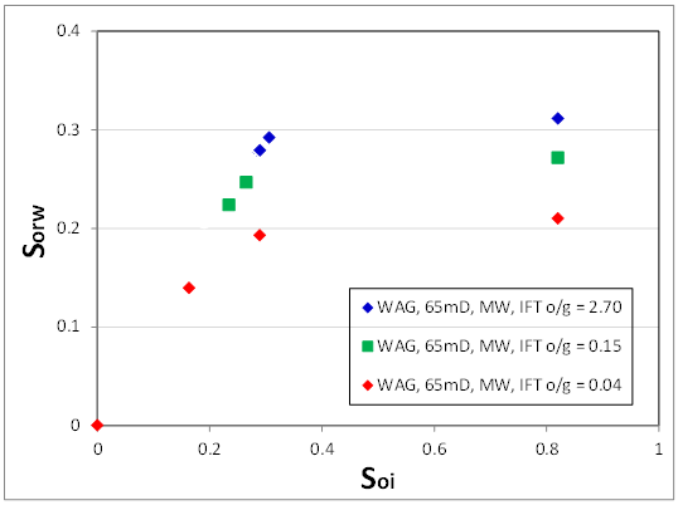

Figure 15: Comparison of trends of the residual oil saturation vs. initial oil saturation during water injection stages of the WAG injections performed at 1840 psia, 1790 psia and 1215 psia (WAG-ID, 65mD, mixed-wet). Note: that zero Soi is just an extrapolated point not actual measured data.

Figure 16 compares the three-phase final trapped gas saturations, as a function of initial gas saturation, obtained from the water injection stages of the three WAG injection tests performed at different gas/oil IFT. The Figure shows that trapped gas saturations (for the same S_{gi}) are larger in the case of immiscible WAG injection compared to the near-miscible WAG injection, and trapped gas saturations for the intermediate IFT lie between these two extreme conditions. This shows that a larger trapped gas saturations do not necessarily mean higher efficiency of WAG injection (considering lower performance of WAG injections at 1790 psia and 1215 psia compared to the one performed at 1840 psia.

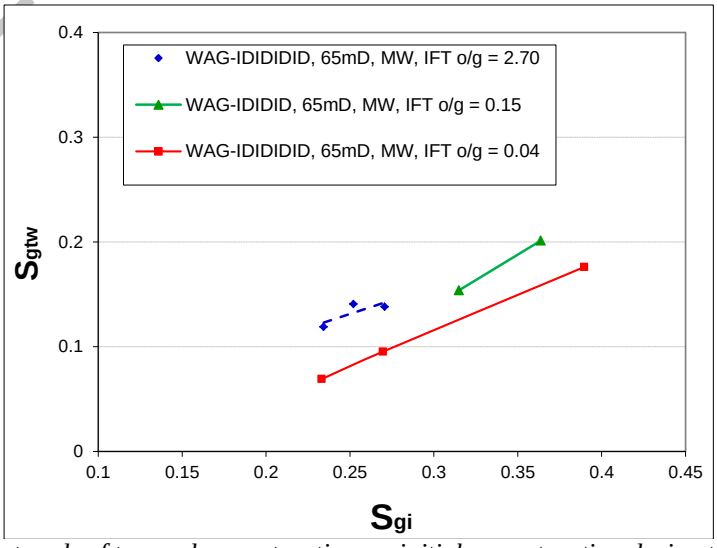

Figure 16: Comparison of the trends of trapped gas saturation vs. initial gas saturation during tertiary water injections of the WAG injections performed at 1840 psia, 1790 psia and 1215 psia (WAG-IDIDID, 65mD, mixed-wet).

To account for the reduction of S_{or} due to trapped gas saturation during water injection, Larsen and Skauge (1998) proposed a linear relationship between residual oil and trapped gas saturation as defined below:

$$S_{orw} = S_{om} - aS_{gt} \quad \text{(Eq. 1)}$$

Where S_{orw} and S_{gt} are residual oil and trapped gas saturations in three-phase flow regime (after water injection periods), S_{om} is the residual oil under the two-phase flow process, achieved by primary waterflooding and "a" is the slope of the linear trends, to be determined by matching experimental data. Figure 17 shows the assessment of this linear type formulation for different WAG-IDIDID injection tests performed at different values of gas/oil IFT. For the case of immiscible condition the "a" is smaller than the one for near-miscible injection, and the "a" parameter for intermediate IFT is very close to the immiscible condition. This shows that "a" parameter is a function of gas/oil IFT and should be obtained for the appropriate system representing the actual reservoir system.

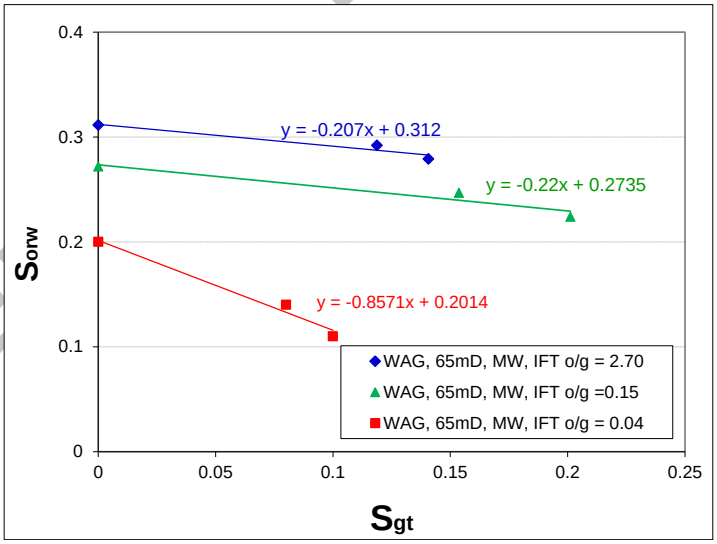

Figure 17: Residual oil saturation, at the end of water injection periods of WAG injection, as a function of trapped gas saturation - for different values of gas/oil IFT (WAG-IDIDID, 65mD, mixed-wet).

Effect of Gas/Oil IFT on the Performance of WAG-DI Injection Scenario

Figure 18 compares oil recovery of the three WAG-DI injection scenarios performed in the 65mD mixed-wet core sample. All these experiments started with a gas injection. As discussed in the previous sections, the performance of the 1st gas injection is lower for the case of immiscible condition (1215

psia) compared to the other two cases (Figure 10). However, oil recoveries at the end of 1st gas injection periods (after 2.68 PV injections) are very close. Nevertheless, at the end of the 1st cycle of WAG-DI injection (i.e., the end of 1st water injection), the performance of the immiscible injection (shown by the dark blue curve) is significantly higher compared to the near-miscible and intermediate IFT injections. In addition, produced oil at the end of 1st cycle of injection, is almost 2.5 % (core PV) higher for the intermediate IFT injection compared to the injection performed at near-miscible condition. To highlight oil production from 1st water injection period and afterwards in the case of these three WAG-DI injections, Figure 19 shows the oil production during 1st waterflooding after 1st gas injection (left graph) as well as oil production from 2nd gas injection and afterwards (right graph). There is a good trend between produced oil in the 1st water injection and the gas/oil IFT. In fact, for this period of injection, the amount of produced oil (in terms of fraction of S_{org}) is larger for the case with higher gas/oil IFT. The same trend observed in the case of presenting the oil production in terms of core PV. Interestingly, after the 1st injection cycle, there is also a trend between gas/oil IFT and the oil recovery, but in the reverse direction (which is more expected). This means that produced oil from 2nd gas injection and afterwards, is significantly larger for the case of near-miscible WAG-DI injection compared to the other two WAG-DI injections performed at higher $IFT_{g/o}$ conditions.

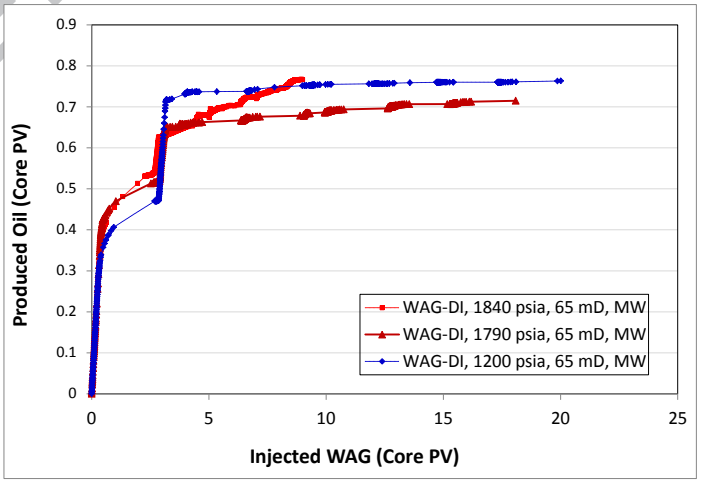

Figure 18: Comparison of produced oil for DIDIDIDI injection scenarios performed at different gas/oil IFT = 2.70, 0.15 and 0.04 mN.m^{-1} (WAG-DIDIDI, 65mD, mixed-wet).

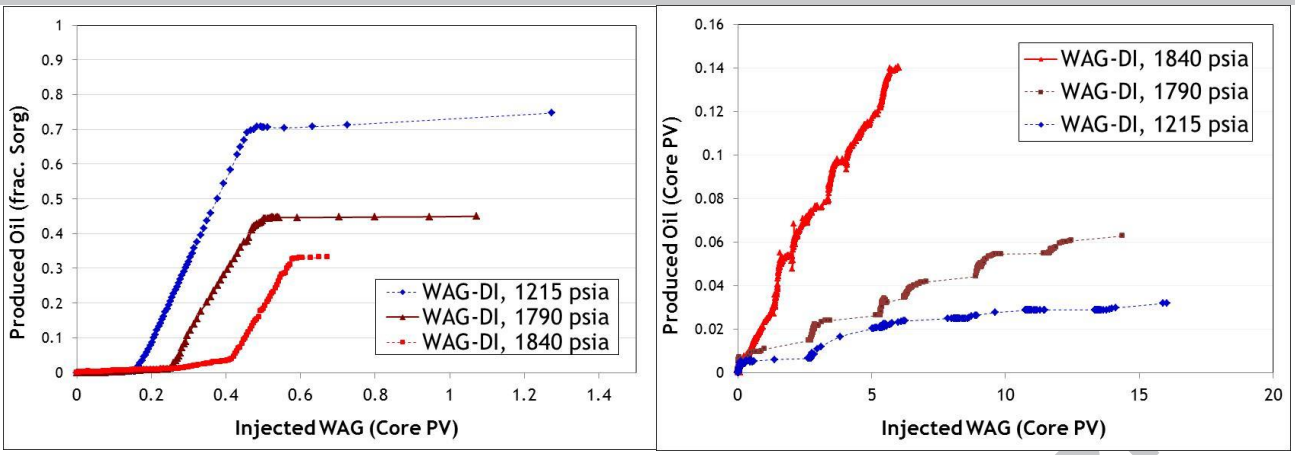

Figure 19: Comparison of produced oil from 1st water injection (left) and afterwards (right) for WAG-DI injection scenarios performed at different gas/oil IFT = 2.70, 0.15 and 0.04 mN.m^{-1} (65mD, mixed-wet).

Figure 20 compares saturations' paths for these DIDIDIDI injections. For the near-miscible injection, during the 1st water injection period there are large changes in water and gas saturations before any significant amount of oil is produced (small changes in oil saturation for this period). Contrary to the near-miscible condition, the water and gas saturations changes during the 1st water injection period in immiscible injection are much less. This means that in the case of immiscible DIDIDIDI injection, water needs to displace less gas before it can be in contact with and displace the oil phase. The saturation path for the intermediate IFT injection lies between these two extremes.

Figure 21 compares the injectivity for the 1st water injection period of immiscible WAG-DIDIDIDI injection, with that of 1st water injection period of immiscible WAG-IDIDIDID injection. Interestingly, although the 1st water injection of DIDIDIDI process involves three-phase flow (water injection in the presence of both oil and gas phases), the injectivity is almost identical to the primary waterflooding (water injection in the absence of gas phase, which is a two-phase flow). Figure 21, middle and bottom charts, show the same comparisons but for the cases of intermediate-IFT and near-miscible WAG injections. The results show that there is a good correlation between gas/oil IFT and the difference between the injectivities for these two water injection periods. The injectivity difference becomes larger as the gas/oil IFT decreases.

Figure 22 compares injectivities for different water injection periods of the WAG-DI performed under gas/oil IFT = 2.70 mN.m^{-1}. The same comparisons are shown in Figure 23 and Figure 24 for WAG-DI

injections performed under gas/oil IFT = 0.15 and 0.04 mN.m^{-1}, respectively. For all systems there is significant loss of injectivity for the later stages of water injection compared to the 1st water injection period. The same behaviour was observed for the cases of WAG-ID injections under high (2.70 mN.m^{-1}) and intermediate (0.15 mN.m^{-1}) gas/oil IFT (Figure 14 middle and bottom graphs). However, for the case of near-miscible WAG-ID injection (Figure 14 top graph) the injectivity loss is not significant compared to its WAG-DI counterpart (Figure 24).

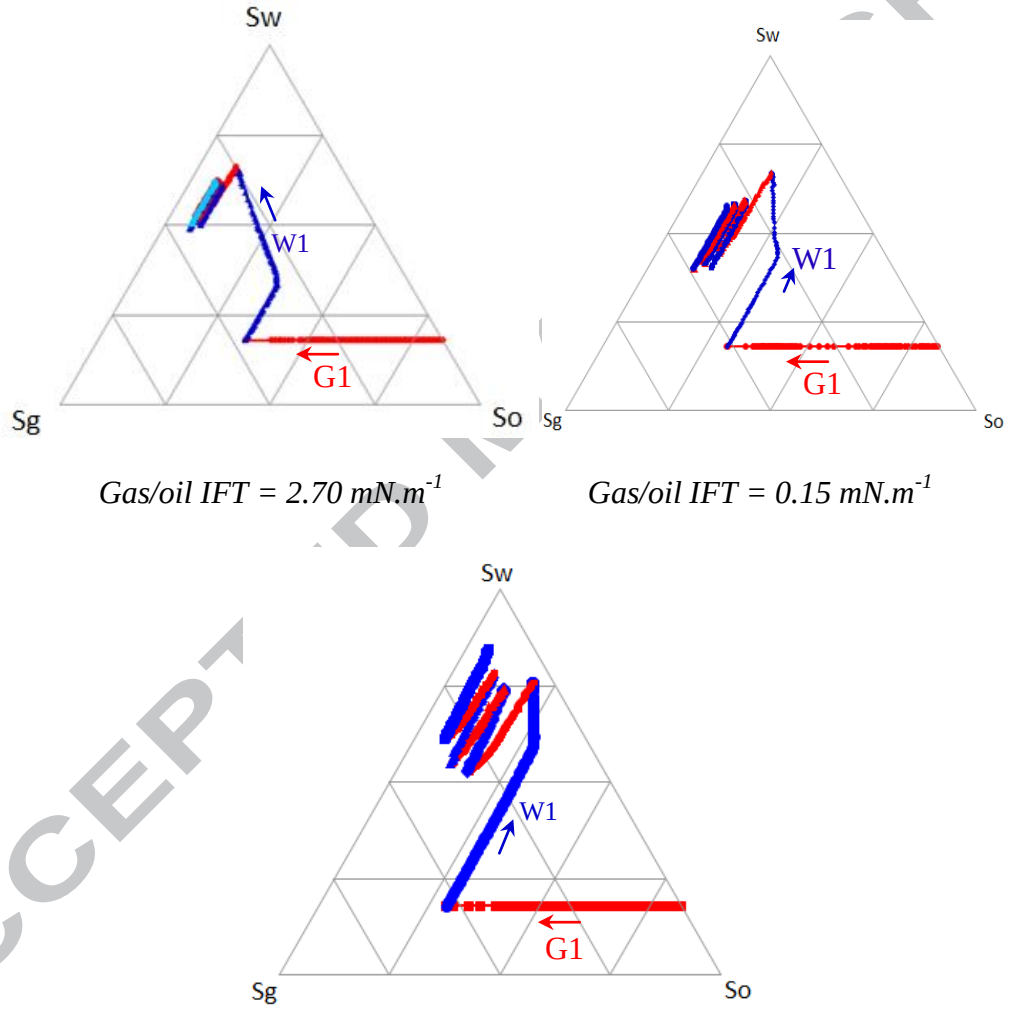

Gas/oil IFT = 2.70 mN.m^{-1}

Gas/oil IFT = 0.15 mN.m^{-1}

Gas/oil IFT = 0.04 mN.m^{-1}

Figure 20: Ternary diagram of saturations changes during WAG-DI injections performed at gas/oil IFT = 2.70, 0.15 and 0.04 mN.m^{-1}; from left and top to bottom: gas/oil IFT = 2.7 mN.m^{-1} ; gas/oil IFT = 0.15 mN.m^{-1} and gas/oil IFT = 0.04 mN.m^{-1} (red: gas injection, blue: water injection;65mD, mixed-wet).

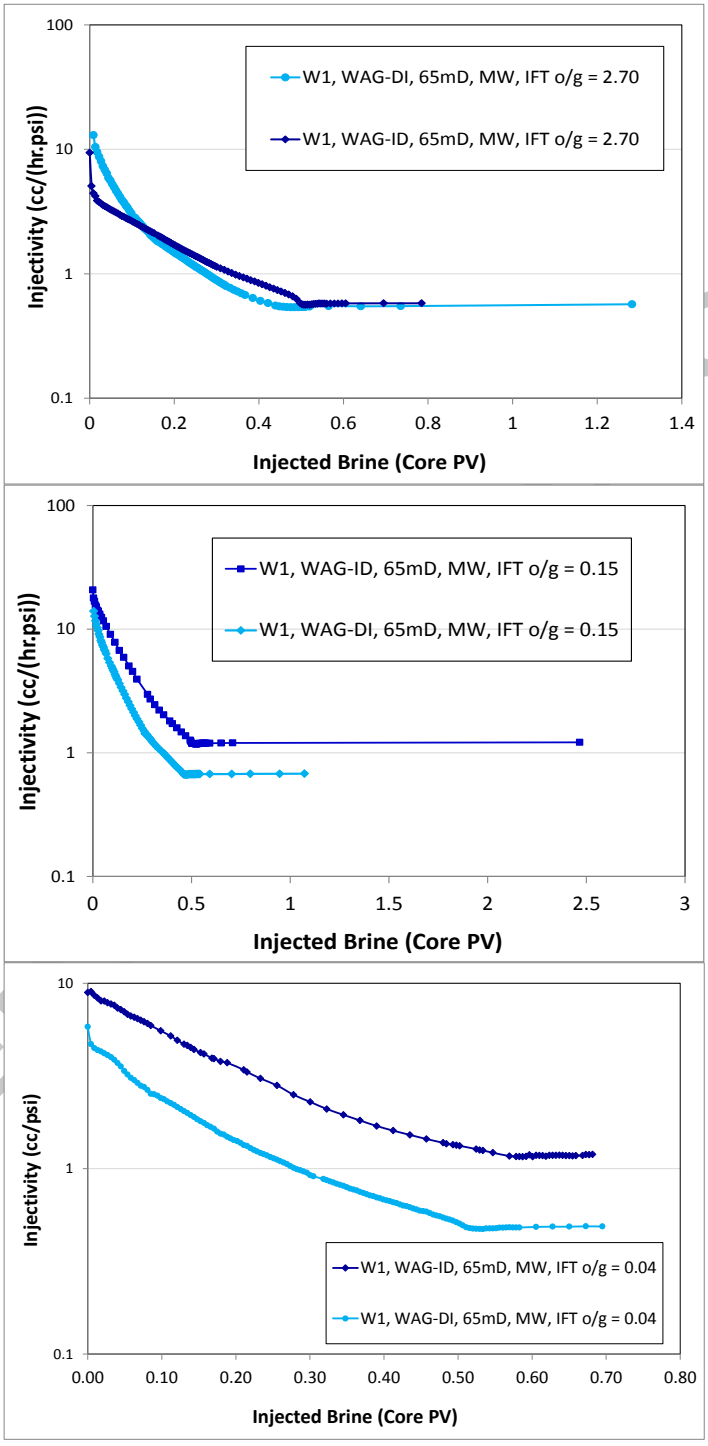

Figure 21: Comparison of injectivities into the core for the 1st water injection of WAG-DIDIDIDI and 1st water injection of the WAG-IDIDIDID injection test; from top to bottom gas/oil IFT = 2.70; 0.15 and 0.04 mN.m^{-1} (65 mD, mixed-wet).

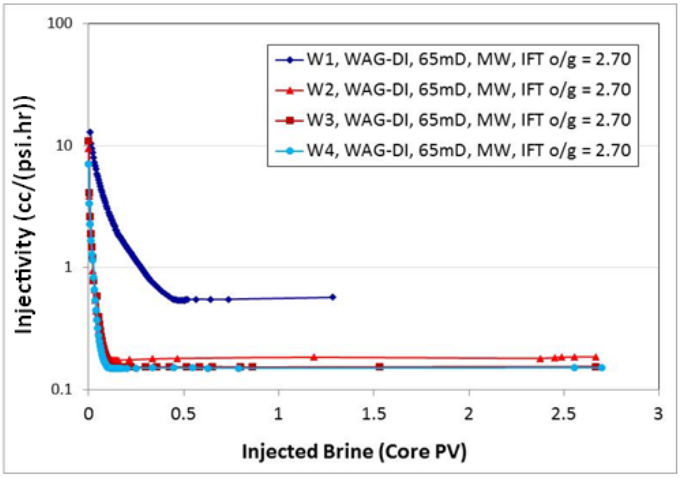

Figure 22: Comparison of injectivities for different water injection periods of WAG-DI injection test (IFT o/g = 2.70 mN.m^{-1}, 65 mD, mixed-wet).

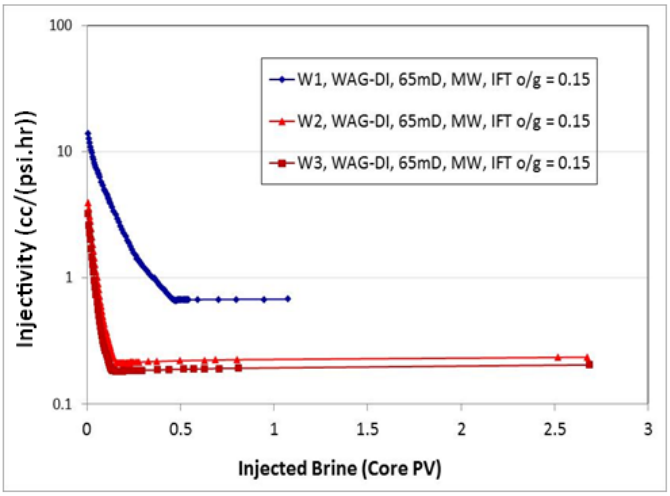

Figure 23: Comparison of injectivities for different water injection periods of WAG-DI injection test (IFT o/g = 0.15 mN.m^{-1}, 65 mD, mixed-wet).

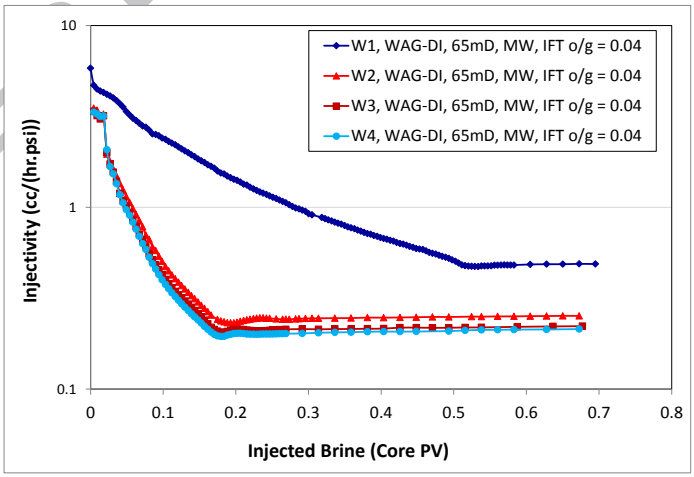

Figure 24: Comparison of injectivities for different water injection periods of WAG-DI injection test (IFT o/g = 0.04 mN.m^{-1}, 65 mD, mixed-wet).

Figure 25 shows the trapped gas saturations at the end of water injection periods of these three WAG-DI injections performed at different gas/oil IFT conditions. For all WAG-DI tests the point with the highest value of S_{gi} corresponds to 1st water injection (W_1). Contrary to the WAG-ID injections (Figure 16), for DIDIDIDI injections, S_{gtw} values are not necessarily higher for higher S_{gi} values. This means that most of trapping models such as Land (which is the base model for S_{gt} calculation in WAG-Hysteresis model), Carlson, and Jerauld 1st and 2nd models are not able of capturing the trend of trapped gas saturations for the case of our DIDIDIDI injections. This is due to the fact that these models are generated based on water-wet systems in which the trapped saturations increases monotonically with increasing the initial non-wetting saturations (Spiteri et al., 2008), which is not the case in our mixed-wet system.

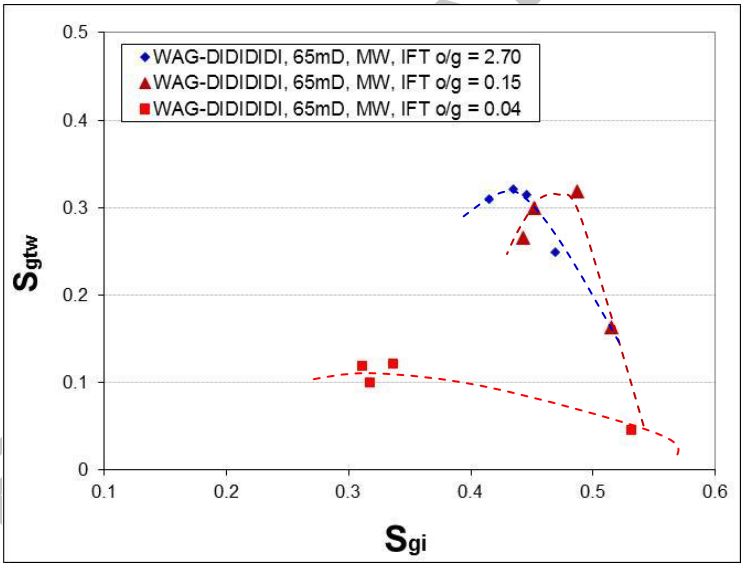

Figure 25: Comparison of the trapped gas saturation vs. initial gas saturation for tertiary waterflooding of WAG-DIDIDIDI injections performed at 1840 psia, 1790 psia and 1215 psia (65mD, mixed-wet, DIDIDIDI).

As a result, we believe that the difference between the trends in Figure 16 and Figure 25 is not only due to the injection sequence but is mostly due to the difference in the range of S_{gi} for these two graphs. Figure 26 shows three-phase trapped gas saturations for both WAG-ID and WAG-DI injections together at near-miscible and immiscible conditions. Interestingly the trends of data (dashed curves) are very similar to the predictions of the Spiteri et al. (2008) trapping model (Figure 27). It should be mentioned

that Spiteri et al. model is based on pore-network modeling not core flood experiments. This model is developed for oil/water system but for a homogeneous porous media, which means that contact angle of the fluids and rock is a constant value for the whole system. This is contrary to what we expect for our rock system in which there are some pores (small pores) which are water-wet, and others (larger pores) which are non-water wet (oil-wet or neutral-wet). In addition, for our system the contact angles might be different in different parts of the same pore (partly water-wet and partly oil-wet). This makes our system more complex and that may explain the observed discrepancy between our experimental trapped oil data and those obtained by the Spiteri et al. model. Another issue is the pore size distribution and pore-network structure. Spiteri et al. pore network model represents Berea sandstone which its pore size distribution and pore-network structure is not the same as our Clashach sandstone. This highlights the need for generalization of trapped phase saturation Spiteri et al. model parameters for different rock types, three-phase flow and different spreading conditions (Fatemi and Sohrabi, 2013d).

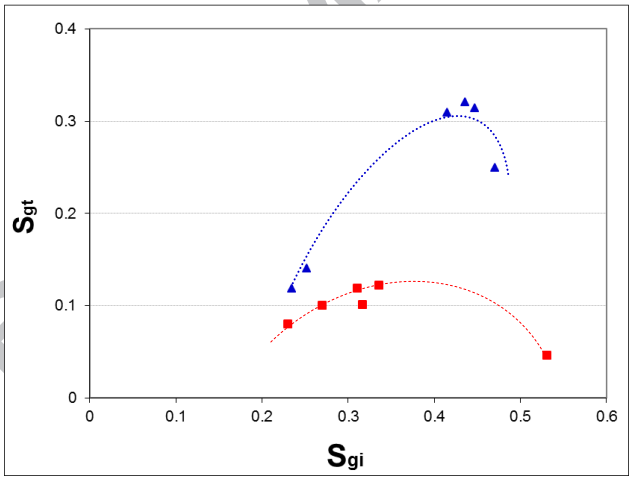

Figure 26: trend of the three-phase trapped gas saturation vs. initial gas saturation for tertiary waterflooding of WAG-DI and WAG-ID injections performed at 1840 psia (red) and 1215 psia (blue) (65mD, mixed-wet).

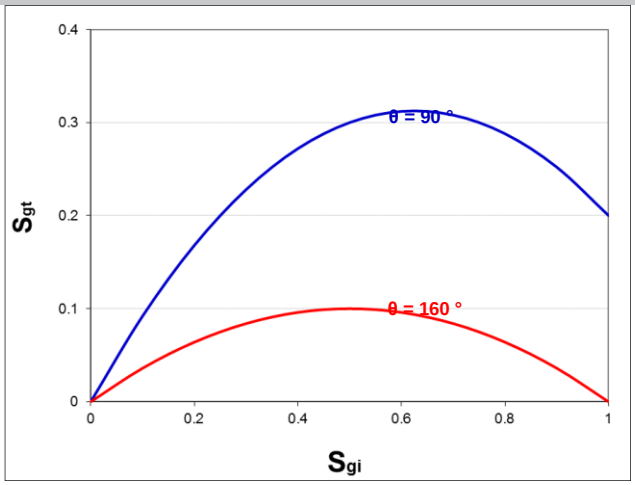

Figure 27: trend of the two-phase trapped gas saturation vs. initial gas saturation as predicted by Spiteri et al. (2008) model for different wettability conditions (contact angles).

Figure 28 shows an assessment of Eq. 1 for the WAG experiments performed in the 65 mD rock under the conditions of different gas-oil IFT and injection strategies. As was mentioned above, this correlation has been suggested to capture the reduction of S_{orw} in the presence of trapped gas. For the case of immiscible condition (bottom chart in Figure 28) the value of "a" in Eq. 1 is larger for the case of WAG-DI injection compared to the WAG-ID injection, which is contrary to the case of near-miscible injections (top chart in Figure 28) where "a" is larger for the case of WAG-ID injection compared to the WAG-DI injection. This shows that in addition to gas/oil IFT dependency (Figure 17), "a" is also injection scenario dependent and should be obtained from the appropriate sequence of fluid injection.

Figure 29, top chart, compares residual oil saturations obtained at the end of water injection stages of the two WAG-ID and WAG-DI injections performed at 1840 psia. The Figure shows that residual oil saturations (at the same S_{oi}) are almost identical for the case of near-miscible DIDIDIDI and IDIDIDID WAG injections. Figure 29, bottom chart, compares similar results but for the case of immiscible WAG injection experiments, which shows significant effect of injection scenario on the trend of residual oil saturation (for the same S_{oi}). This is especially true for medium to large S_{oi} values. Figure 29, middle chart, shows that the effect of injection scenario at gas/oil IFT = 0.15 $mN.m^{-1}$ is between these two extremes. It should be mentioned that the residual oil saturation corresponding to the highest initial oil saturation (S_{oi} = 82 %) is in fact the two-phase trapped oil saturation at the end of primary

waterflooding. This point can be assumed to be the limit of the three-phase trapped oil saturation in which initial gas saturation approached zero (since in the presence of immobile water saturation (S_{wim} = 18 %) and S_{oi} = 82 % there will be no gas in the system).

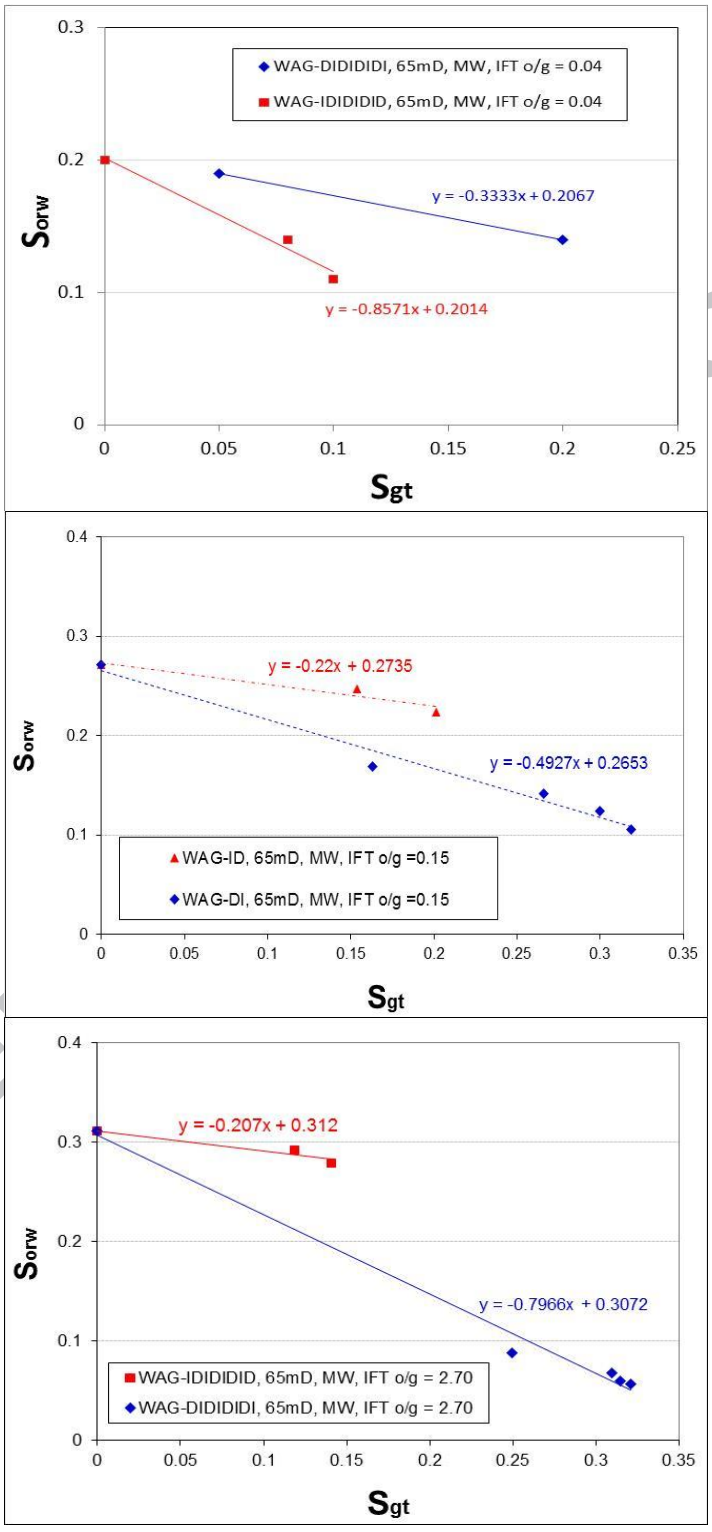

Figure 28: Effect of injection scenario on the trend of residual oil saturation at the end of water injection periods as a function of trapped gas saturation. From top to bottom: gas/oil IFT = 0.04 mN.m^{-1}; 0.15 mN.m^{-1} and 2.70 mN.m^{-1} (WAG-ID and WAG-DI, 65 mD, mixed-wet).

Effect of Gas/Oil IFT on the Performance of SWAG Injection (Q_g/Q_w=1.0)

In this section we compare the results of the two SWAG injection tests performed under near-miscible and immiscible conditions. Both experiments have been performed in 65 mD mixed-wet sample with Q_g/Q_w = 1.0. Although the extension of the period of SWAG injection for ultra-low gas/oil IFT system is not as long as the immiscible case, but the pressure drop trends before and after water breakthrough are similar to those of the immiscible SWAG test. Figure 30 shows the saturation variations for three phases in the SWAG test performed at near-miscible conditions. With the start of the test, water and gas saturations have increased along with the reduction of the oil saturation (oil production). Once the gas BT happened, the gas saturation started to slightly decrease while the production of oil (and hence, decrease in oil saturation) and increase in water saturation continued. It is worth mentioning that, the same trend was observed in the case of near-miscible SWAG injection test performed with Q_g/Q_w = 0.25 (Sohrabi and Fatemi, 2012). After water BT, water and oil saturations decreased slightly while gas saturation inside the core increases. Comparing Figure 30 and Figure 9 it is obvious that the qualitative difference between the two IFT systems is in the period between the two BT points (gas and water BTs). For the case of immiscible system, there is almost no gas production (gas saturation is stable) in this period while there is 0.05 PV (11 cm^3) gas production in the case of near-miscible system.

Figure 31 shows the ternary diagram of the saturations path during immiscible SWAG (I-SWAG) and near-miscible SWAG (nM-SWAG) tests, which clearly highlights the differences between the two systems. Figure 32 shows the amount of produced oil for I-SWAG and nM-SWAG tests. Gas breakthrough happened earlier (in terms of injected SWAG PV) for the case of nM-SWAG injection compared to the I-SWAG test. Water BT happened almost at the same time (in terms of injected SWAG PV) for the two SWAG tests. Figure 33 compares the injectivity of the two SWAG tests, which shows better injectivity (Q_{inj}/Dp) for the case of nM-SWAG test compared to the I-SWAG injection.

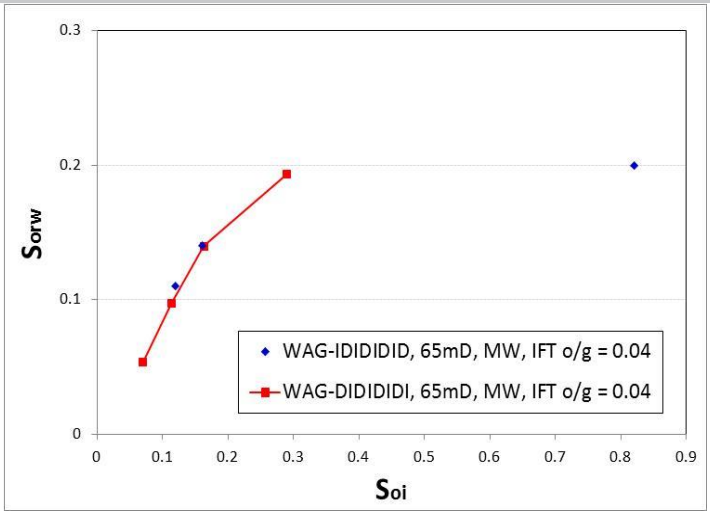

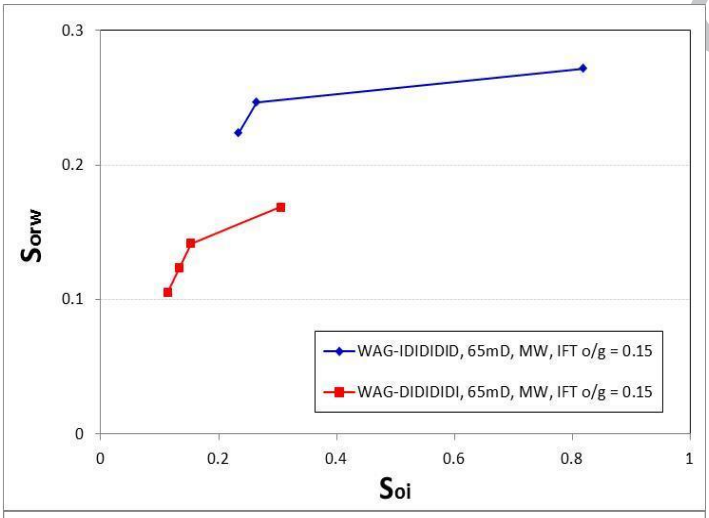

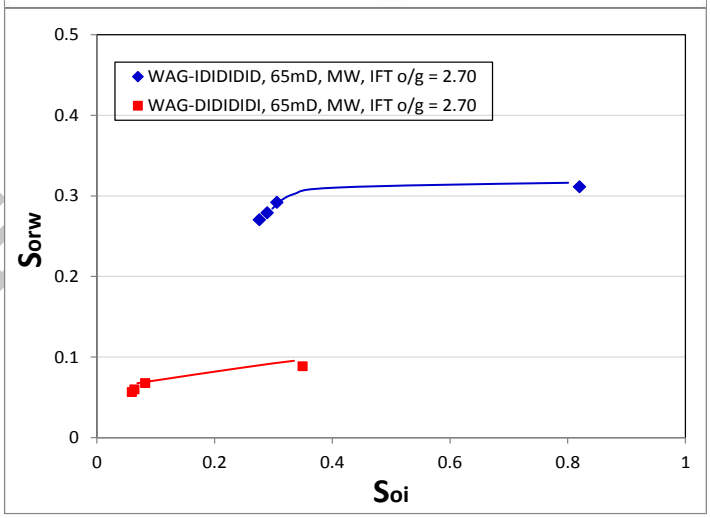

Figure 29: Comparison of the residual oil saturation vs. initial oil saturation for water injections of the WAG injections performed at different gas/oil IFT. From top to bottom gas/oil IFT = 0.04 mN.m^{-1}; 0.15 mN.m^{-1} and 2.70 mN.m^{-1}(WAG-ID and WAG-DI, 65 mD, mixed-wet).

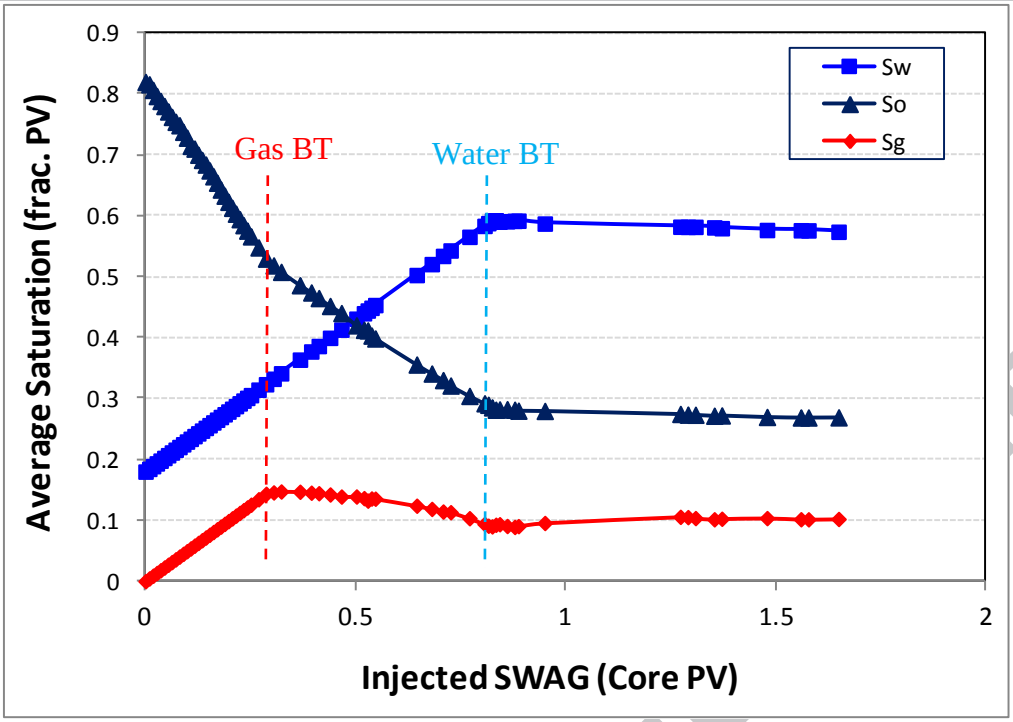

Figure 30: Average saturations inside the core for SWAG injection (Near-Miscible gas/oil system, IFT = 0.04 mN.m^{-1}, Qg/Q_w=1.0, 65mD, Mixed-Wet)

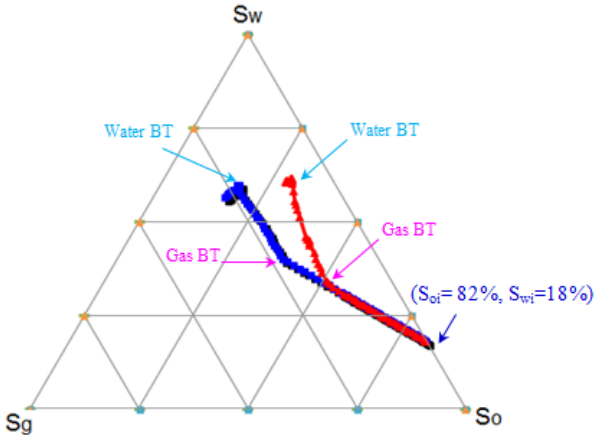

Figure 31: Saturations paths for SWAG injection tests performed at near-miscible, IFT = 0.04 mN.m^{-1}, (red curve) and immiscible IFT = 2.7 mN.m^{-1}, (dark blue) gas/oil conditions (Q_g/Q_w=1.0, 65mD, Mixed-Wet)

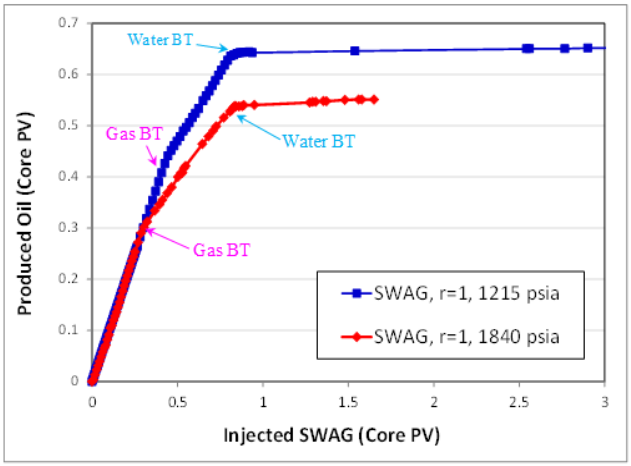

Figure 32: Produced oil for SWAG injections performed at near-miscible, IFT = 0.04 mN.m^{-1}, and immiscible gas/oil conditions, IFT = 2.7 mN.m^{-1}, (Q_g/Q_w=1.0, 65mD, Mixed-Wet)

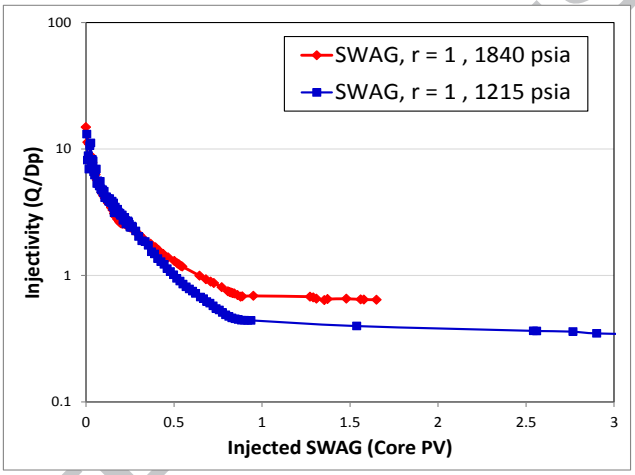

Figure 33: Injectivity for two SWAG injections performed at near-miscible, IFT = 0.04 mN.m^{-1}, and immiscible, IFT = 2.7 mN.m^{-1} gas/oil conditions (Q_g/Q_w=1.0, 65mD, Mixed-Wet)

Effect of Gas/oil IFT on the Oil Recovery Order of Injection Scenarios

In this section we compare the performance of different injection scenarios, i.e., primary water flooding, primary gas injection, WAG-ID (which started with primary waterflooding) and WAG-DI (which started with primary gas injection) and SWAG at each of immiscible and near-miscible conditions. It should be borne in mind that in our investigation, the SWAG tests were not considered as methods for improving recovery after the primary water flooding since in these experiments the SWAG tests began from the start of oil production. Figure 34 compares the performance of the different injection scenarios performed at the ultra-low gas/oil IFT. Figure 35 shows a similar comparison for the case of high gas/oil

IFT system. It can be concluded that gas/oil IFT, for the system under investigation here, has significantly affected the oil recoveries obtained by different injection scenarios (in terms of oil recovery). For the case of near-miscible conditions the order in terms of higher oil recovery is WAG_{ID}> WAG_{DI}>> WF > SWAG > GI (in which " >" means larger than, and " >> " means extremely larger than) however for the case of immiscible system this order is rearranged to WAG_{DI}> SWAG >> WAG_{ID}> WF > GI. Note that for although in the case of 1840 psia, GI outperforms WF after 8 pore volumes injections. Due to economical and practical concerns this makes WF a better injection scenario since it achieves the same recovery factor in just 0.7 or so PV injection.

A potential problem with SWAG injection is the adverse effect of one injection fluid on the injectivity of the other. Figure 36 compares injectivity during the SWAG injection test with those of the 1st water injection periods in WAG-ID (two-phase waterflooding) and WAG-DI (water injection after two-phase gas injection) for the case of immiscible system. Figure 37 shows a similar comparison for the case of near-miscible system. For the case of immiscible system, SWAG injectivity is less compared to the two water injection periods, however, for the case of near-miscible system, SWAG injectivity lies between the two water injections. This shows less injectivity problems in the case of near-miscible system compared to the immiscible condition, however, as discussed earlier the performance of SWAG injection was better for the I-SWAG compared to the nM-SWAG test.

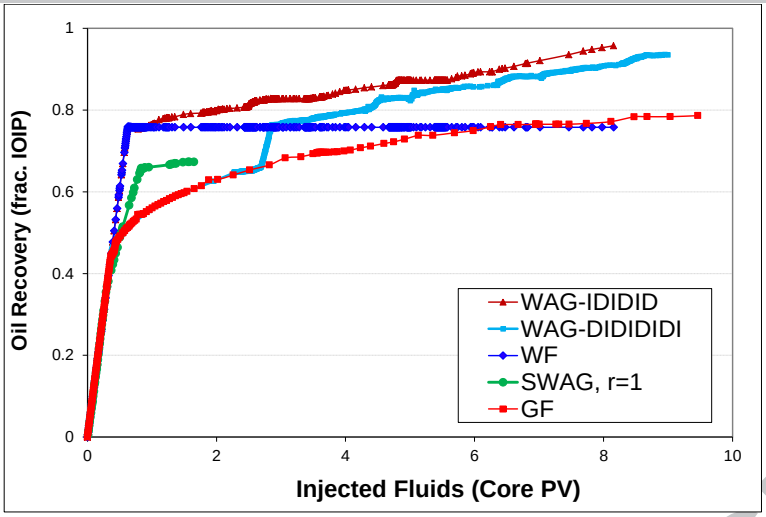

Figure 34: comparison of the oil recovery for different injection scenarios (WF, GI, WAG-ID, WAG-DI and SWAG) all performed at near-miscible gas/oil condition (1840 psia, 65mD, Mixed-Wet)

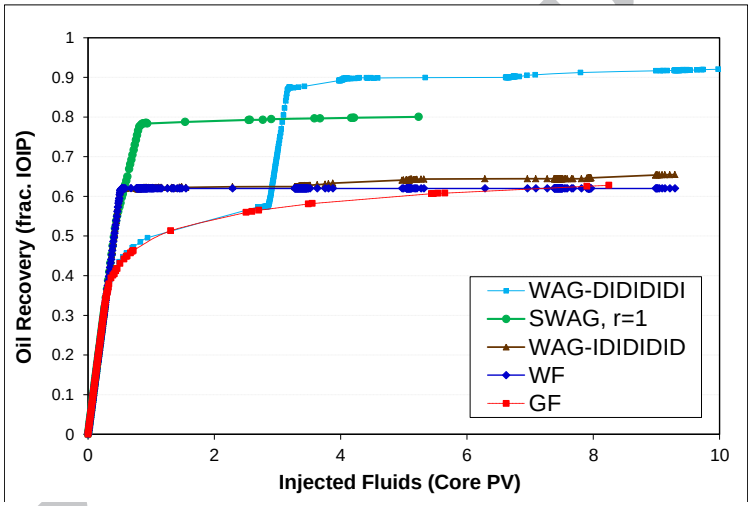

Figure 35: comparison of the recovered oil for different injection scenarios (WF, GI, WAG-ID, WAG-DI and SWAG) performed at immiscible gas/oil condition (1215 psia, 65mD, Mixed-Wet)

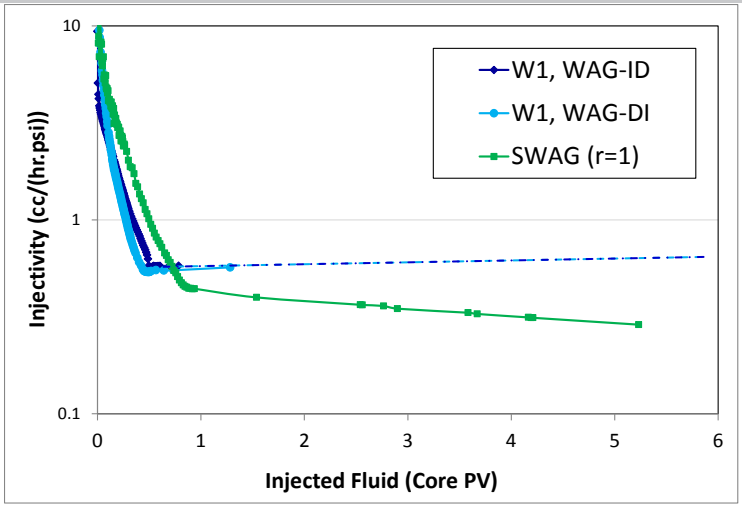

Figure 36: Comparison of the values of injectivity into the core for the 1st water injection of WAG-DIDIDIDI, 1st water injection of the WAG-IDIDIDID injection test and SWAG injection (gas/oil IFT = 2.70 mN.m^{-1}, 65 mD, mixed-wet).

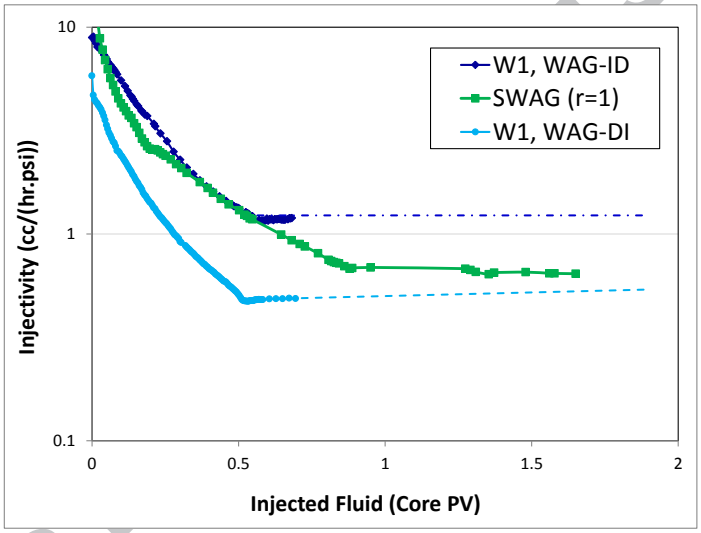

Figure 37: Comparison of the values of injectivity into the core for the 1st water injection of DIDIDIDI, 1st water injection of the WAG-IDIDIDID injection test and SWAG injection (gas/oil IFT = 0.04 mN.m^{-1}, 65 mD, mixed-wet).

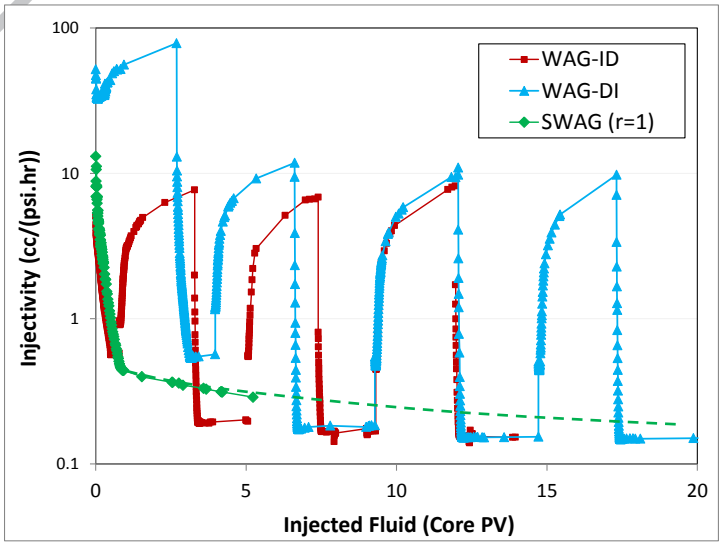

Figure 38: Comparison of the values of injectivity into the core for the WAG-DI, WAG-ID and SWAG injection (gas/oil IFT = 2.70 mN.m^{-1}, 65 mD, mixed-wet).

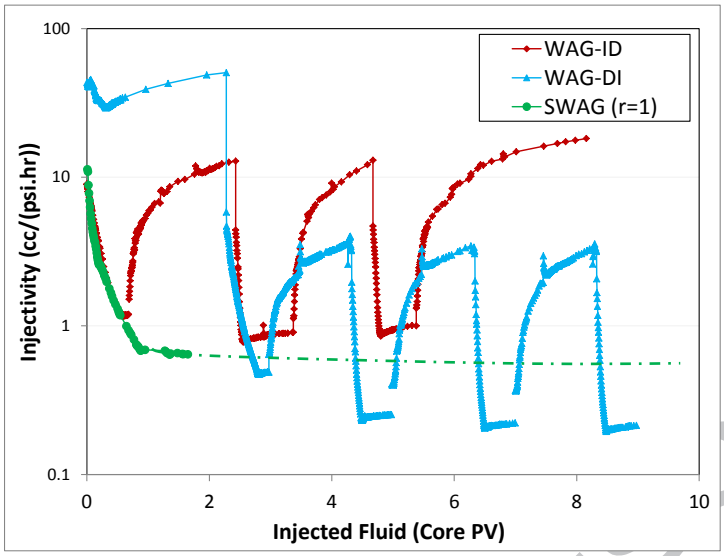

Figure 39: Comparison of the values of injectivity into the core for the WAG-DI, WAG-ID and SWAG injection (gas/oil IFT = 0.04 mN.m^{-1}, 65 mD, mixed-wet). Note: for the case of SWAG experiment injectivity is equal to the total injection rate (qw+qg) divided by Dp.

Figure 38 compares the values of injectivity of the SWAG injection test with those of the WAG-ID and WAG-DI tests under immiscible conditions. Figure 39 shows a similar comparison for the case of near-miscible system. For both systems, as expected, WAG injections show significant fluctuations in the values of injectivity during alternation between water and gas injection. The values of injectivity improve during gas injection periods but drop significantly over water injection periods. Green dashed curves in these Figures show the extrapolated trend of SWAG injectivity. In the case of immiscible system, the order of the injection scenarios based on higher values of (better) injectivity is: WAG_{DI} >> WAG_{ID} >> SWAG, however poor recovery performance of the WAG_{ID} injection (no significant oil production after 1st WF) rules out this injection scenario. In the case of near-miscible system, the order of the injection scenarios based on higher values of injectivity is: WAG_{ID} >> WAG_{DI} >> SWAG, which is the same order based on higher oil recovery.

Regarding the case with gas/oil IFT = 0.15 mN.m^{-1}, Figure 40 compares different injection scenarios for this intermediate gas/oil IFT conditions. Although the oil recovery in the primary gas injection is lower than that in the primary waterflooding, yet both the rate of oil production and ultimate oil recovery achievable at the end of the 1st cycle of injection, are higher in the WAG-DI case (i.e., the test starting

with gas injection) compared to the WAG-ID injection (i.e., the test starting with water injection). This is the same trend observed for the case of different injection scenarios performed at immiscible gas/oil IFT (Figure 35).

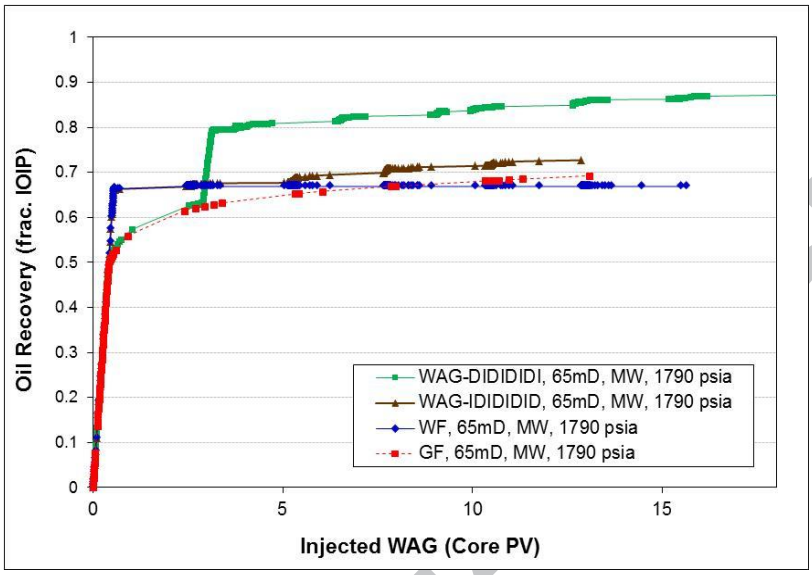

Figure 40: Assessment of different injection scenarios performed at 1790 psia (gas/oil IFT = 0.15 mN.m^{-1}, 65mD, mixed-wet).

Table 6: Summary of the coreflood experiments performed in 65 mD mixed-wet sandstone at 1840 psia (Gas/Oil IFT = 0.04 mN.m^{-1}, S_{wim} = 0.18).

Experiment	***Recovery Factor (% IOIP)***
Gas Injection	79
Water Injection	77
WAG-ID	97
WAG-DI	95
SWAG $_{(Qg/Qw=1)}$	67

Table 7: Summary of the coreflood experiments performed in 65 mD mixed-wet sandstone at 1790 psia (Gas/Oil IFT = 0.15 mN.m^{-1}, S_{wim} = 0.18).

Experiment	***Recovery Factor (% IOIP)***
Water Injection	67
Gas Injection	69
WAG-ID	73
WAG-DI	87

Table 8: Summary of the coreflood experiments performed in 65 mD mixed-wet sandstone at 1215 psia (Gas/Oil IFT = 2.70 mN.m^{-1}, S_{wim} = 0.18).

Experiment	***Recovery Factor (% IOIP)***
Water Injection	62
Gas Injection	63
WAG-ID	67
WAG-DI	93
SWAG $_{(Qg/Qw=1)}$	80

Conclusions

Table 6 to Table 8 summarize the recovery performance of various injection scenarios at different gas/oil IFTs. Based on the presented results and discussion in this work following conclusions are obtained.

- Comparison of the performance of the extended gas injections for ultra-low (gas/oil IFT = 0.04 mN.m^{-1}), intermediate (0.15 mN.m^{-1}) and high IFT (2.70 mN.m^{-1}) conditions in 65 mD mixed-wet system, shows that the oil recovery is lower for extended gas injection performed at higher gas/oil IFT conditions. The effect of gas/oil IFT was more pronounced in 1000 mD mixed-wet core than it was in 65 mD core. This means that the improvement in recovery obtained by reducing gas/oil IFT (by increasing pressure or gas enrichment) would be more significant for high permeability rocks than low permeability ones. As explained in text, this is the direct result of capillary forces being less effective at lower gas/oil IFT.
- Our results show that for mixed-wet rocks, at all different gas/oil IFT (pressure) levels investigated, oil recovery by gas injection is lower than that obtained by waterflooding. This conclusion is in contrast with the results of a similar comparison for near miscible gas injection (oil/gas IFT=0.04 mN.m^{-1}) in water-wet system which outperforms the waterflooding at the same pressure. High performance of waterflooding in the mixed-wet system is due to lower degree of snap-off mechanism in non-water wet pores of this system compared to the water-wet condition.

- In mixed-wet system and for the case of ultra-low gas/oil IFT, WAG-ID injection considerably improved oil recovery over waterflood recovery. The improved oil recovery by WAG-ID injection was marginal at immiscible condition, compared to the significant additional oil production obtained under near-miscible WAG injection. Nevertheless, the performance of WAG injection is still better than that of gas injection at later stages of injection, where gas injection outperforms waterflood. For the intermediate gas/oil IFT conditions in which oil and gas viscosities are very close to the near-miscible condition but the gas/oil IFT is one order of magnitude higher, WAG injection recovery profile is closer (although slightly improved) to the immiscible case. High performance of the WAG-ID in mixed-wet systems is due to good recovery performance of the initial waterflooding. Nevertheless, the high performance of nM-WAG injection highlights the importance of gas/oil IFT effect on the performance of this WAG injection scenario.

- Contrary to the marginal additional oil recovery obtained during WAG-ID at immiscible condition, the WAG-DI injection scenario showed significantly more oil production during the first WAG cycle water injection (after 1stgas injection). As a result, under immiscible conditions, DIDIDID injection scenario significantly outperformed WAG-ID. The same trend observed at intermediate gas/oil IFT condition. These observations at high and intermediate IFT conditions were in contrary to the results of near-miscible WAG injections, where WAG-ID outperformed DI injection scenario and the difference between them was relatively small after 1st cycle of WAG injection. High recovery performance of WAG-DI is mostly due to the 1st waterflooding after initial gas injection. Our results show that there is a good trend between produced oil in the 1st water injection and the gas/oil IFT, in which the amount of produced oil (in terms of fraction of S_{org}) is larger for the case with higher gas/oil IFT. As explained in the text, higher recovery performance of the 1st waterflooding is due the fact that water shall displace less gas before it can be in contact with and displace the oil phase. Nevertheless, the ultimate performance of WAG-DI injection was less sensitive to the gas/oil IFT compared to the WAG-ID injection scenario.

- Comparison of the amount of recovered oil by different injection scenarios (WAG, SWAG, gas injection and waterflood) performed at ultra-low gas/oil IFT and high gas/oil IFT (2.70 $mN.m^{-1}$) reveals that the order of injection scenarios (in terms of produced oil) is different for these two systems. For near-miscible system (1840 psia), the order of injection strategies from highest to lowest oil recovery is; WAG_{ID}, WAG_{DI}, water flooding, SWAG and gas injection. For the case of immiscible system (1215 psia), the order of injection strategies from highest to lowest oil recovery is; WAG_{DI}, SWAG, WAG_{ID}, water flooding, and gas injection.

- Comparing the injectivity data obtained during tertiary water injected after the first gas injection period (three-phase) with those of secondary water injection (two-phase) shows that in both WAG experiments (1840 psia, $IFT_{o/g}$ = 0.04 $mN.m^{-1}$ and 1200 psia, $IFT_{o/g}$ = 2.70 $mN.m^{-1}$), the injectivity of water decreases when water injection resumes after the first gas injection. However, this reduction in injectivity is much larger for the case of immiscible WAG injection compared to near-miscible one. As a result, loss of injectivity in immiscible WAG injections (e.g., WAG using Nitrogen) is expected to be more than that in low IFT WAG injection (e.g., WAG injection using CO_2 or high pressure hydrocarbon gas). This highlights the importance of oil/gas IFT (gas type and enrichment) as a design criterion in tertiary gas or WAG injection.

- For the case of near-miscible system, from injectivity point of view, the order of injection scenarios from high to low are WAG_{ID}, SWAG and WAG_{DI}. For the immiscible system the order is: WAG_{DI}, WAG_{ID}, and SWAG injections.

- Trapped gas saturations are larger in the case of immiscible WAG-ID injection ($IFT_{g/o}$ = 2.7 $mN{\cdot}m^{-1}$) compared to the near-miscible WAG-ID injection ($IFT_{g/o}$ = 0.04 $mN{\cdot}m^{-1}$), and trapped gas saturations for the intermediate pressure ($IFT_{g/o}$ = 0.15 $mN{\cdot}m^{-1}$) lie between these two conditions. This shows that larger trapped gas saturations do not necessarily mean higher efficiency of the WAG injection (considering lower performance of WAG injections at 1790 psia and 1215 psia compared to the one performed at 1840 psia.

- Contrary to the WAG-ID injections, for WAG-DI injection scenarios, S_{gtw} values are not necessarily larger for higher S_{gi} values. Considering the mixed-wet condition of the core, we believe that the observed difference between WAG-DI and WAG-ID is simply due to lager S_{gi} values experienced in the WAG-DI compared to the WAG-ID in our experiments (large initial non-wetting saturation is where the non-monotonic behaviour of S_{nwt} vs. S_{nwi} happens). Non-monotonic trend might have been observed for WAG-ID if core had experienced such high large S_{gi} values as those observed in WAG-DI. As a result in the case mixed-wet system WAG-DI injection scenario, most of the trapping models such as Land, Carlson, and Jerauld 1st and 2nd models are not able to capture the trend of trapped gas (non-wetting phase) saturations for the initially high non-wetting saturations.

- It should be noted that the oil recovery values obtained in our experiments are purely the results of direct displacement of the oil. Since the fluids had been pre-equilibrated, the effect of other mechanisms such as; solution gas drive, swelling, mass transfer, phase changes etc. had been excluded (to be able to investigate the effect of hysteresis on relative permeabilities). Also the effect of gravity segregation that may be important at field scale had not played a role in our experiments. The contribution of these factors may result in additional oil recovery by immiscible WAG injection in a real reservoir.

Acknowledgements

This work was carried as part of the Improved Characterisation of Three-phase Flow and WAG Injection joint industry project (JIP) at Heriot-Watt University. The project is currently supported equally by: ADNOC, Galp Energia, Maersk oil, Petrobras, Premier Oil, Shell, Schlumberger , Total, and Woodside Energy which is gratefully acknowledged.

References

Alkhazmi B., Sohrabi M., Farzaneh A., (2017): An Experimental Investigation of the Effect of Gas and Water Slug Size and Injection Order on the Performance of Immiscible WAG Injection in a Mixed-Wet System, SPE-187537-MS, presented at SPE Kuwait Oil and Gas Show and Conference, 15-18 October, Kuwait City, Kuwait.

Awan A.R., Teigland R., and Kleppe J., (2008): A Survey of North Sea Enhanced-Oil-Recovery Projects Initiated During the Years 1975 to 2005, SPE Reservoir Evaluation & Engineering, Volume 11, Number 3, pp. 497-512.

Blunt M.J., (2000): An empirical model for three-phase relative permeability, SPE Journal, Volume 5, Issue 4, pp. 435–445.

Caudle, B. H. and Dyes, A. B.: 1958, Improving miscible displacement by gas–water injection, Petroleum Transactions, AIME, Volume 213, pp. 281-283.

Christensen, J. R., Stenby, E. H., and Skauge, A., (2001): Review of WAG Field Experience, SPE Reservoir Evaluation & Engineering, Volume 4, Number 2, pp. 97-106.

Duchenne S., de Loubens R., Joubert T., (2016): Extended Three-Phase Relative Permeability Formulation and its Application to the History-Matching of Multiple WAG Corefloods Under Mixed-Wet Conditions, SPE-183257-MS, presented at Abu Dhabi International Petroleum Exhibition & Conference, 7-10 November, Abu Dhabi, UAE

Element D.J., Masters J.H.K., Sargent N.C., Jayasekera A.J. and Goodyear S.G., (2003): Assessment of Three-phase Relative Permeability Models Using Laboratory Hysteresis Data, SPE 84903, Proceedings of the SPE International Improved Oil Recovery Conference in Asia Pacific, Kuala Lumpur, Malaysia.

Fahimpour J. and Jamiolahmady M., (2014): Impact of Gas-Condensate Composition and Interfacial Tension on Oil-Repellency Strength of Wettability Modifiers, Energy & Fuels, Volume 28, Issue 11, pp 6714-6722.

Fatemi S.M., (2015): Multiphase Flow and Hysteresis Phenomena in Oil Recovery by Water Alternating Gas (WAG) Injection, PhD Thesis, submitted to the Institute of Petroleum Engineering at Heriot-Watt University, Edinburgh, UK.

Fatemi S.M.; Sohrabi M.; (2012a): Cyclic Hysteresis of Three-Phase Relative Permeability Applicable to WAG Injection: Water-Wet and Mixed-Wet Systems under Low Gas/Oil IFT, SPE-159816, SPE Annual Technical Conference and Exhibition (ATCE), 8 - 10 October, San Antonio, Texas, USA.

Fatemi S.M.; Sohrabi M.; (2012b): Experimental and Theoretical Investigation of Water/Gas Relative Permeability Hysteresis: Applicable to Water Alternating Gas (WAG) Injection and Gas Storage Processes, SPE-161827, Abu Dhabi International Petroleum Exhibition and Conference, 11-14 November, Abu Dhabi, UAE.

Fatemi S.M.; Sohrabi M.; Jamiolahmady M.; Ireland S., (2012): Experimental and Theoretical Investigation of Oil/Gas Relative Permeabilities Hysteresis in the Presence of Immobile Water: under Low Oil/Gas IFT and Mixed-Wet Conditions, *Energy Fuels*, Volume 26, Issue 7, pp 4366–4382.

Fatemi S.M. and Sohrabi M.; (2013a): Experimental Investigation of Near-Miscible Water-alternating-gas (WAG) Injection for Water-wet and Mixed-wet Systems, SPE Journal, Volume 18, Number 1, pp. 114-123.

Fatemi S.M.; Sohrabi M; (2013b): "Cyclic Hysteresis of Three-Phase Relative Permeability Curves Applicable to WAG Injection under Low Gas/Oil IFT: Effect of Immobile Water Saturation, Injection Scenario and Permeability", SPE-164918, 75th EAGE Conference & Exhibition incorporating SPE EUROPEC, 10-13 June, London, United Kingdom.

Fatemi S.M.; Sohrabi M.; (2013c): Recovery Mechanisms and Relative Permeability for Gas/Oil Systems at Near-Miscible Conditions: Effects of Immobile Water Saturation, Wettability, Hysteresis and Permeability, Energy & Fuels, 27 (5), pp 2376–2389.

Fatemi S.M.; Sohrabi M.; (2013d): Experimental and Theoretical Investigation of Two- and Three-Phase Oil and Gas Trapping under Low Oil/Gas IFT Conditions: Applicable to Water Alternating Gas (WAG) Injection, SPE-166193, SPE Annual Technical Conference & Exhibition, 30 September – 2, New Orleans, LA, USA.

Fatemi S.M.; Sohrabi M; (2013e): Experimental and Numerical Investigation of the Impact of Design Parameters on the Performance of WAG and SWAG Injection in Water-Wet and Mixed-Wet Systems, SPE-165286, SPE Enhanced Oil Recovery Conference, 2-4 July, Kuala Lumpur, Malaysia.

Fatemi S.M.; Shahrokhi O., Sohrabi M., Ahmad. K., (2015): Experimental Investigation of Oil Recovery from Carbonate Reservoir Rocks under Oil-Wet Condition: Waterflood, Gas Injection, SWAG and WAG Injections, SPE-177641, presented at Abu Dhabi International Petroleum Exhibition and Conference (ADIPEC) to be held 9-12 November, Abu-Dhabi, UAE.

Fatemi S.M.; Sohrabi M.; (2018): Relative Permeabilities Hysteresis for Oil/Water, Gas/Water and Gas/Oil Systems in Mixed-wet Rocks, Journal of Petroleum Science and Engineering, Volume 161, pp. 559-581.

Gozalpour, F., Danesh, A., Todd, A.C. et al. (2005): Viscosity, density, interfacial tension and compositional data for near critical mixtures of methane + butane and methane + decane systems at 310.95 K, Fluid Phase Equilibria, Volume 233, Issue 2, pp. 144–150.

Henderson G.D., Danesh A., Tehrani D.H., and Al-Kharusi B., (2000): The Relative Significance of Positive Coupling and Inertial Effects on Gas Condensate Relative Permeabilities at High Velocity, SPE-62933-MS, SPE Annual Technical Conference and Exhibition, 1-4 October, Dallas, Texas.

Kulkarni M.M. and Rao D.N.; (2005): Experimental investigation of miscible and immiscible Water-Alternating-Gas (WAG) process performance. Journal of Petroleum Science and Engineering, Volume 48, Issue 1-2, pp. 1-20.

Shahrokhi O., Fatemi S.M., Sohrabi M., Ireland S., Ahmed K., (2014):Assessment of Three Phase Relative Permeability and Hysteresis Models for Simulation of Water-Alternating-Gas (WAG) Injection in Water-wet and Mixed-wet Systems, SPE-169170, SPE Improved Oil Recovery Symposium held in

Tulsa, Oklahoma, USA, 12–16 April.

Sohrabi M., Tehrani D.H., Danesh A., Henderson G.D., (2004): Visualization of Oil Recovery by Water-Alternating-Gas Injection Using High-Pressure Micromodels, SPE-89000, SPE Journal, Volume 9, Number 3, pp. 290-301.

Sohrabi M., Danesh A. and Jamiolahmady M., (2008): Visualisation of Residual Oil Recovery by Near-miscible Gas and SWAG Injection Using High-pressure Micromodels, Transport in Porous Media, Volume 74, Number 2, pp. 239-257.

Sohrabi M.; Fatemi S.M.; (2012): Experimental Investigation of Oil Recovery by Different Injection Scenarios under Low Oil/Gas IFT and Mixed-Wet Condition: Water-Flood, Gas Injection, WAG and SWAG Injection, SPE-161074, Abu-Dhabi International Petroleum Exhibition and Conference, 11-14 November, Abu Dhabi, UAE.

Spiteri E.J., Juanes R., Blunt M.J., Orr F.M.; (2008): A New Model of Trapping and Relative Permeability Hysteresis for All Wettability Characteristics, SPE Journal, Volume 13, Number 3, pp. 277-288.

Suicmez V.S., Piri M. and Blunt M.J., (2007): Pore-scale Simulation of Water Alternate Gas Injection, Transport in Porous Media, Volume 66, Number 3, pp. 259-286.

- Reliable laboratory data on Gas injection, waterflooding, WAG and SWAG injections under realistic reservoir conditions

- coreflood experiments carried out at three different levels of gas/oil IFT namely, ultra-low, intermediate, and high gas/oil IFT values of 0.04, 0.15, and 2.70 mN.m-1 in mixed-wet rocks.

- novel insights into the mechanisms involved in three-phase flow taking place in WAG injection for different gas/oil IFT values and different WAG injection scenarios.

- The presented experimental data can be used to assess the validity of three-phase relative permeability and hysteresis models and/or generate novel or modified methodologies.